Shallow Landslide Risk Assessment of the Westerly Bluffs of the 7.5-minute Freeland Quadrangle, Whidbey Island, WA

Evelyn Conrado

A report prepared in partial fulfillment of
the requirements for the degree of

Master of Science
Earth and Space Sciences: Applied Geosciences

University of Washington

June, 2015

Internship coordinator:
Kathy Troost

Reading committee:
Alison Duvall
Steven Walters

MESSAGe Technical Report Number: 025

Abstract

Landslides often occur on slopes rendered unstable by underlying geology, geomorphology, hydrology, weather-climate, slope modifications, or deforestation. Unfortunately, humans commonly exacerbate such unstable conditions through careless or imprudent development practices. Due to local geology, geography, and climatic conditions, Puget Sound of western Washington State is especially landslide-prone. Despite this known issue, detailed analyses of landslide risks for specific communities are few. This study aims to classify areas of high landslide risk on the westerly bluffs of the 7.5 minute Freeland quadrangle based on a combined approach: mapping using LiDAR imagery and the Landform Remote Identification Model (LRIM) to identify landslides and implementation of the Shallow Slope Stability Model (SHALSTAB) to establish a landslide exceedance probability. The objective is to produce a risk assessment from two shallow landslide scenarios: (1) minimum bluff setback and runout and (2) maximum bluff setback and runout. A simple risk equation that takes into account the probability of hazard occurrence with physical and economic vulnerability (van Westen, 2004) was applied to both scenarios. Results indicate an estimated total cost of $32,600,000 would occur from a shallow landslide with a setback of 12 m and a runout of 235 m.

Table of Contents

Acknowledgements

I would like to acknowledge a small group of people who all brought their own contribution and made this project possible; Alison Duvall for her review and intellectual contribution and mentoring; Steven Walters for his review contribution and GIS assistance; Stephen Slaughter for his LRIM model; and Harvey Greenberg for his time and assistance with SHALSTAB. The SHALSTAB aspect of this project would not have been possible without him.

Introduction

Landslides have caused widespread damage in Washington State. Thus understanding how and why landslides occur is therefore fundamental in developing mitigation techniques and determining future hazards (Washington Division of Geology and Earth Resources, www.dnr.wa.gov/ResearchScience/Topics/GeologicHazardsMapping/Pages /landslides.aspx). Landslides are usually related to instabilities in slopes caused by underlying geology, geomorphology, hydrology, weather-climate, or deforestation, and can be triggered by volcanic eruptions, earthquakes, precipitation, slope modification, undercutting or a combination of all of these (May, 2013; Highland, 2004). Landslides that occur on bluffs and hillsides surrounding Puget Sound pose a serious hazard to people, property, utilities, transportation, and businesses (U.S. Geological Survey, 2014) due to high population density. Many large prehistoric landslides, which could be activated during wet periods or a seismic event, are found along the Puget Sound shoreline (Shipman, 2004). Despite this danger, demand for waterfront and bluff property is high, driven primarily by access to the water and unimpeded views of the Sound with development occurring at the base of steep coastal bluffs (Shipman, 2004). Therefore, humans play a primary role in hillslope instability through careless or imprudent development practices (Shipman, 2004).

In Island County, particularly on Whidbey Island, geology, geomorphology, hydrology, precipitation, slope modification, and undercutting from waves all play a role in landslide susceptibility along the bluff. Island County encompasses 221 miles of shoreline, 112 miles of which are considered unstable (Shipman, 2004). The subsurface geology of 2Island County consists of the Vashon till, Esperance outwash, and Lawton clay (Figure 1). The Esperance outwash lies on top of the Lawton clay with the over-steepened bluff slopes exhibiting slopes greater than 60 degrees (Swanson, personal communication). This is important because a common driver of upslope failure is the contact between the advance outwash, which is permeable, and clay deposits, which are impermeable. The Vashon till often unconformably overlays the Esperance outwash, and is usually highly resistant to erosion and typically forms steeper cliffs and slopes (Shipman, 2004). The

presence of these distinct stratigraphic elements leads to complex bluff profiles containing both steep and gradual segments. This stratigraphy also impacts the hydrologic characteristics that influence mass-wasting mechanisms (Shipman, 2004). On southern Whidbey Island, the Lawton clay forms relatively shallow aquicludes (Swanson, personal communication). The advance outwash unit continually unravels as it dries out, causing colluvium to accumulate at the base of the slope where it is further mobilized by either creep or landslide processes (Swanson, personal communication). This process is evident in mapped geologic deposits showing prevalent Holocene to late Pleistocene landslide deposits (Qls) on the bluffs of Whidbey Island, particularly on the Freeland quadrangle (Figure 1).

Human impact in the form of slope modification has also been a contributor to instability along the bluffs of Whidbey Island. In the 1950s and 1960s, numerous residential developments on Whidbey Island were created by constructing bulkheads on the beach below a high bluff and then using hydraulic methods to wash bluff material in as landfill (Shipman, 2004). This activity resulted in rows of homes at water level, constructed on unengineered hydraulic fill, and located at the base of unstable bluffs 40 – 70 m high (Shipman, 2004). Surface runoff and subsurface saturation are highly sensitive to the abundance and type of vegetation, especially on steep slopes, and land development and clearing of vegetation can result in changes in subsurface hydrology that increase slope failure likelihood (Shipman, 2004).

The present study focuses on the shallow landslide susceptibility of the westerly bluffs of the 7.5-minute Freeland quadrangle on Whidbey Island (Figure 2). The study was conducted by creating two shallow landslide scenarios to determine the minimum and maximum risk consisting of: (1) minimum bluff setback and runout and (2) maximum bluff setback and runout. Based on the results from these two scenarios, I then applied a simple risk formula (Van Westen, 2004) (see equation 4) to calculate risk per digital elevation model (DEM) cell grid (200 m × 200 m). The results of this study will benefit the residents living along the bluffs by highlighting areas prone to landsliding and

assessing potential social and economic losses as may occur following a future slope failure.

Scope of Work

This project aims to classify areas of high landslide risk on the westerly bluffs of the 7.5 minute Freeland quadrangle on the basis of mapped landforms using LiDAR imagery, the Landform Remote Identification Model (LRIM) and the Shallow Slope Stability Model (SHALSTAB) to identify hazardous areas. SHALSTAB was also used to establish a landslide exceedance probability. LiDAR imagery allows identification of landforms indicative of past landslide events and to verify instability. LRIM is used to identify hazardous areas based on the desired calibrations of slope and curvature (Washington Division of Geology and Earth Resources, 2014), and SHALSTAB is used to identify areas at risk of instability depending on critical rainfall (Montgomery et al., 2001). I correlate the Shallow Slope Stability Model results from my field site with previous studies of Seattle (Coe et al., 2000) in order to determine the annual exceedance probability for the field area. I focus on two shallow landslide scenarios to produce a risk assessment. My final results estimate the cost and damage associated with each scenario.

Background

Hazard vs. Risk

For this study, both a hazard and risk assessment was conducted; therefore, it is important to identify the difference between the two. Hazard is defined as a condition with the potential for causing an undesirable consequence (Technical University of Catalonia, 2011). Risk, on the other hand, is defined as a measure of the probability and severity of an adverse effect to property, and is often estimated by the product of probability multiplied by consequences (Technical University of Catalonia, 2011).

Significant landslides in Washington State

Between the winter of 1995 and 1999, the Puget Sound region experienced extremely heavy precipitation resulting in the initiation of shallow landslides and debris avalanches (Shipman, 2001). The heavy precipitation came in both the form of extremely intense periods of rainfall over several days and in the form of prolonged wet conditions over many months (Shipman, 2001). During the winter of 1996-1997, two disaster declarations, which included landslides, were made due to heavy rains. The following counties were affected by such landslides: Clallam, Island, Jefferson, King, Kitsap, Mason, Pierce, and Snohomish. Following this disaster the Federal Emergency Management Agency (FEMA) started making geotechnical expertise available to property owners in order to identify appropriate actions for minimizing additional losses or risks (Shipman, 2001). During 1998-1999, the Puget region experienced the wettest winter on record. By February of 1999, several very large, deep-seated landslides began to move (Shipman, 2001). Most of these documented slides occurred in developed areas or in areas where development had recently been proposed, and damages consisted of roads, structures, and utilities (Shipment, 2001).

In March 2014, the Oso Landslide struck the community of Oso in Snohomish County, Washington, occurring along the North Fork Stillaguamish River where earlier landslides had been documented (Geotechnical Extreme Events Reconnaissance, 2014). The landslide initiated within an approximately 200 m high hillslope and transitioned into a catastrophic debris flow with an overall size of approximately 7.6 million cubic meters (Geotechnical Extreme Events Reconnaissance, 2014). The debris flow inundated a neighborhood (Steelhead Haven) of about 35 single-family residences, claimed the lives of 43 people, and caused significant economic losses estimated at more than $50 million (Geotechnical Extreme Events Reconnaissance, 2014). The location of the Oso Landslide is the site of an ancient landslide where the slopes have failed many times since the 1930s. Most recently before the 2014 event, the so-called Hazel Landslide occurred in 2006, at the same site, travelling over 100 m and ultimately blocking the North Fork Stillaguamish River (Geotechnical Extreme Events Reconnaissance, 2014).

Within the 7.5-minute Freeland quadrangle, no major landslides since 2013 have occurred, though older landslides are identified by the Washington Department of Natural Resources (WADNR) geologic map and the State of Washington Department of Ecology Coastal Zone Atlas slope stability map. In contrast, other bluffs on Whidbey Island have experienced recent landslides. In March 2013, for instance, the Ledgewood-Bonair Landslide on Whidbey Island occurred as a small portion of a much larger landslide complex. The dimensions of the landslide were approximately 335 m long and about 91 m into Puget Sound with a volume of mobilized material greater than 200,000 cubic yards (Slaughter et al., 2013). The larger landslide complex is approximately 2.4 km long, and may date back as much as 11,000 years. The Ledgewood-Bonair Landslide was likely a reactivation of a small portion of the prehistoric complex (Slaughter et al., 2013). The landslide observations made consisted of an uplifted pre-existing beach (high as 9 m above shore) at the toe of the slide, which suggested a movement of a deep-seated plane located below sea level. The toe zone consisted of extensive deformation and the landslide body was hummocky with jack-strawed trees throughout. An access road located mid slope was shifted about 24 m down vertically and to the west. The headscarp appeared vertical to sub-vertical and exposed the glacial geology of the area. The top of the scarp averaged 61 m above sea level and contained colluvial wedges. The Ledgewood-Bonair Landslide is still susceptible to additional landslide movement in the toe and body area due to wave and tidal action eroding the toe. The headscarp will also be subjected to erosion from calving of debris (Slaughter et al., 2013). A total of five residences were yellow tagged by Island County due to life safety considerations (Geotechnical Engineering Services, 2013). Another slide known as the North Driftwood Way Landslide, occurred just north of and on the same large landslide complex in the late 1980s. Two homes were destroyed by the slide. This slide area was considered “quiet” for about 8 to 10 years until 2012, when several episodic movement starting occurring requiring roadway repairs (Geotechnical Engineering Services, 2013).

Shallow Landslide Models

The Landform Remote Identification Model (LRIM) is a computer-based screening tool used to identify Forest Practices rule-identified landforms recognized as potential source

areas of management-related shallow landslide initiation (Washington State Department of Natural Resources, 2010). Forest Practices rule-identified landforms, six statewide landforms identified as high hazard due to their instability, include (1) inner gorges, (2) convergent headwall, (3) bedrock hollows, (4) toes of deep-seated landslides with slopes greater than 65%, (5) ground water recharge areas for glacial deep-seated landslides, and (6) outer edges of meander bends along valley walls or high terraces of unconfined meandering streams (Serdar, 2007). LRIM is a geographic information system (GIS)-based model that uses slope angle and slope convergence, derived from LiDAR digital elevation models, to identify landforms commonly recognized as shallow landslide source areas (Washington State Department of Natural Resources, 2010).

The Shallow Slope Stability Model (SHALSTAB) is a physical model that uses ArcINFO and GRID software to map the pattern of shallow slope instabilities (Dietrich and Montgomery, 1998). The model combines hydrology to a limit-equilibrium slope stability model to determine the critical steady-state rainfall required to trigger slope instability at any point in a given landscape (Montgomery et al., 2001). Montgomery et al. (2001) applied their shallow landslide model in the city of Seattle. Digital elevation models (DEMs) at three resolutions, 30 m, 10 m, and 1.5 m, were used to generate predicted patterns of potentially unstable ground to apply the relative slope stability model (Montgomery et al., 2001). SHALSTAB was run using the critical rainfall (Q_c) equation given by

$$Q_c = \frac{T \sin\theta}{(a/b)} \left[\frac{C'}{\rho_w g z \cos\theta \tan\phi} + (\rho_s / \rho_w)[\tan\theta / \tan\phi] \right] \qquad (1)$$

for cohesionless soils, where ρs is the saturated bulk density of the soil, g is gravitational acceleration, ρw is the density of water, ϕ is the friction angle of the soil (Montgomery et al., 2001; Montgomery and Dietrich, 1994), and C' is the apparent cohesion (Montgomery et al., 2001; Montgomery et al., 1998).

For all three model runs a single set of parameters that reasonably estimate general properties of glacial deposits in Seattle (Montgomery et al., 2001; Koloshi et al., 1989)

were applied: ($\rho s/\rho w$) = 2.0, C = 2 kPa, ϕ = 33°, and T = 65 m^2/day (Montgomery et al., 2001). The model's performance varied with DEM cell size, but the areas identified as high risk occupy less than 1 percent of the area of the City of Seattle. The results from the model were correlated with historic landslides from a 100-year record of 1,358 landslide locations (Montgomery et al., 2001). The areas predicted to be at risk for shallow landslide initiation corresponded well with the map pattern of historic landslide locations (Montgomery et al., 2001). The results of this study show that in Seattle, slope gradient is more important than drainage area as a control on potentially unstable ground (Montgomery et al., 2001). Also, landslide hazards in Seattle are strongly associated with a small area of Seattle that can be objectively identified in spite of the hydrologic complexity of the urban environment (Montgomery et al., 2001). The SHALSTAB results for the City of Seattle are important for this study as they will be used to correlate between the Freeland quadrangle SHALSTAB results to provide a landslide exceedance probability.

Geologic Setting

Regional geology

The Puget Lowland is a structural basin in western Washington bounded by Mesozoic and Tertiary rocks of the Cascade Range on the east and accreted Cenozoic rocks of the Olympic Mountains on the west (Booth et al., 2003). The Puget Lowland has been repeatedly occupied by glaciers (Shipman, 1963) that have advanced south into the lowlands at least six times (Booth et al., 2003). The most recent ice sheet advance was the Puget Lobe during the Vashon advance (ca. 14,500 ^{14}C yr B.P.) (Troost and Booth, 2008) extending south of Olympia in the Puget Sound, and a separate lobe extended westward along the Strait of Juan de Fuca (Shipman, 1963; Booth, 1994) (Figure 3). During glaciation, the ice carried clastic material from the mountains of British Columbia. Underneath the ice, subglacial drainage was carving deep erosional troughs (Troost and Booth, 2008). During interglaciations, the glacial sediments were reworked by streams in the Puget Lowland and introduced to compositionally distinct clastic

materials derived from the Cascade Range and Olympic Mountains (Troost and Booth, 2008).

The sequence of glacial deposition and erosion is both horizontally and vertically gradational and time-transgressive (Troost and Booth, 2008). When the Puget Lobe dammed the north flowing streams within the lowland, a system of proglacial lakes developed where glacial lacustrine sediment, Lawton Formation were deposited (Troost and Booth, 2008). The Lawton Formation consists of the Lawton clay, laminated silt and clay (Troost and Booth, 2008). As the Puget Lobe continued to advance south, the Esperance Formation (^{14}C yr. B.P.) (Booth et al., 2003; Millineux et al., 1965; Porter and Swanson, 1998) was deposited into the proglacial lakes and onto upland surfaces. The Esperance Formation consists of an advance outwash unit of sand and gravel (Troost and Booth, 2008). Then, as the lobe advanced south and overrode the outwash apron, the Vashon till was deposited (Troost and Booth, 2008). As the Puget Lobe retreated, recessional outwash consisting of sandy outwash and muddy lacustrine analogous to those formed during the ice advance was deposited (Troost and Booth, 2008). The present-day Puget Lowland is dominated by areas of nondeposition, soil formation, or minor upland erosion (Troost and Booth, 2008).

Tectonic setting

The Puget Lowland is a zone of active tectonic stresses driven by the eastward subduction of the Juan de Fuca plate, northward migration of the Pacific plate, and extension farther east of the Basin and Range Province (Booth et al., 2004; Wells et al., 1998). The dominant tectonic pattern is that of convergence along a north-trending subduction zone with a series of west- to northwest-trending faults crossing the lowland (Booth et al., 2004; Johnson et al., 1994); among these faults is the southern Whidbey Island Fault, one of many active and potentially hazardous structures.

Gower et al. (1985) first postulated the southern Whidbey Island Fault (SWIF) (Figure 4) as an unexposed fault based on magnetic and gravity anomalies, evidence of displacement of Quaternary strata in boreholes, and minor faulting exposed in upper

Quaternary sediments (Johnson et al., 1996). Gower et al. (1985) also inferred that the SWIF is a northwest-trending southern fault, based on two major crustal blocks observed in the south Whidbey Island area (Johnson et al., 1996). Johnson et al. (1996) describe evidence for recent movement on the SWIF based on the following evidence: (1) offset and disrupted upper Quaternary strata imaged on seismic-reflection profiles; (2) borehole data (supplied by W. W. Rau, 1992) suggesting as much as 420 m of structural relief on the Tertiary-Quaternary boundary in the fault zone; (3) several meters of displacement evident in boreholes and minor faulting exposed in upper Quaternary sediments; (4) late Quaternary folds with limb dips of as much as ≈9°; (5) large-scale liquefaction features in upper Quaternary sediments within the fault zone; and (6) minor historic seismicity. Based on this, the SWIF is likely capable of generating large earthquakes ($Ms \geq 7$) and must be considered in evaluation of Whidbey Island/Puget Sound seismic hazards (Johnson et al., 1996). The SWIF is important for this study because strands of the fault have been identified within the 7.5-minute Freeland quadrangle.

Methods

For this project, I conducted several analyses that focus on the westerly bluffs of the 7.5-minute Freeland Quadrangle (Figure 2). I mapped landslide complexes using LiDAR data as a starting place and then applied LRIM to the same areas to identify locations of future potential landslides based on topography. This was conducted in order to identify prior landsliding and instability. I then did a separate analysis of future potential landsliding using SHALSTAB. This analysis takes into account both topography as well as hydrology in predicting slope stability. SHALSTAB is meant to predict shallow slope failures (Deitrich and Montgomery, 1995). In addition, I assessed the economic value of property within the field site by creating a GIS database for Island County properties. Finally, I calculated landslide risk using the probability of landslide occurrence and property values as inputs.

GIS data sources

The LiDAR data used for mapping landslides were obtained from the Puget Sound LIDAR Consortium as a 6-foot hillshade and bare-earth digital elevation model (DEM) acquired during 2000-2005 (PSLC, 2015). Data were presented and projected in Washington State Plane North Coordinate System, NAD 1938. The LiDAR data used for LRIM and SHALSTAB were obtained from the Puget Sound LIDAR Consortium by Island County Public Works as a 3-foot bare-earth DEM acquired 2014 (PSLC, 2015). These data were projected in Washington State Plane North Coordinate System, NAD 1983. I also used Washington State Department of Natural Resource (WADNR) 1:24,000 scale landslides and landform database, to verify past landslides along the bluffs of Whidbey Island.

Mapping landforms using LiDAR imagery

Landslide mapping was conducted using GIS by visually evaluating topographic characteristics indicative of landslides, such as scarps, hummocky topography, convex and concave slope areas, midslope terraces, and offset drainage (Schulz, 2007). Evidence of scarps and hummocky topography is clear within the southwest Whidbey Island field site (Figure 5). I mapped all identified features into a polygon feature class using ArcGIS software. To improve identification of these features, I created a series of hillshade maps from digital elevation data (Table 1).

Table 1. Hillshade layers created based on varying altitude and z-factor

Hillshade	Azimuth	Altitude	z-factor
1	315	45	1
2	315	90	10

In order to check the landslide mapping, I compared the results of my mapped landslide polygons with the Coastal Zone Atlas and with the WADNR landslides and landform database. The 1:100,000 slope stability map from the State of Washington Department of Ecology Coastal Zone Atlas shows relative stability of coastal slopes, as interpreted by geologists based on aerial photographs, geology maps, topography, and field observations (Dept. of Ecology https://fortress.wa.gov/ecy/coastalatlas/tools/Map.aspx). The slope

stability map identifies unstable slides, old unstable slides, and recent unstable slides. WADNR's landslide and landform database includes 1:24,000 scale landslides, which delineates landslides as identified by field geologists mapping surficial geology (Washington Division of Geology and Earth Resources, 2014). In order to verify the landslide areas, I overlaid polygon features from each of the different sources.

Landform Remote Identification Model (LRIM)

The Landform Remote Identification Model (LRIM) is a GIS screening tool used by Washington State Forest Practice to identify potential source areas of shallow landslide initiation (Washington State Department of Natural Resources, 2010). The primary data set used for LRIM is a 3-foot bare-earth DEM clipped to my specified study area in the southwest region of Whidbey Island. LRIM is run in a GIS (such as Esri's ArcGIS) using slope convergence (as measured via planform curvature) and percent slope as inputs. A curvature analysis was performed to capture the influences of convergence and divergence of flow. I then performed a focal statistics analysis on the plan curvature layer in order to smooth out the microtopography features. The mean plan curvature was created within a 3x3 cell rectangular neighborhood window. The LRIM output was created using raster algebra and inputting the following formulas:

(percent slope >= 68) * (smooth plan curvature <= -1)

(percent slope >= 40) * (smooth plan curvature <= -1)

The output identifies the hazard areas based on these calibrated threshold values. For this project I decided to use the requirements used by WADNR rule-identified landforms (Sedar, 2007) for forest practice and Island County's land development standards (Island County, Washington-Code of Ordinances, 2015) (Table 2) in an attempt to capture steeper slopes.

Table 2. LRIM threshold values for varying percent slope for WADNR and Island County standards

Thresholds	Percent Slope	Plan Curvature
WADNR	≥ 68	≤ -1
Island County	≥ 40	≤ -1

Shallow Slope Stability Model (SHALSTAB)

The Shallow Slope Stability Model (SHALSTAB) is a physical model that maps the pattern of shallow slope instabilities using ArcINFO and GRID software (Dietrich and Montgomery, 1998). SHALSTAB combines a hydrologic model with a limit-equilibrium slope stability model to determine the critical rainfall required to trigger slope instability (Montgomery et al., 2001). The hydrologic model divides a catchment into topographic elements defined by intersection of contours and flow tube boundaries orthogonal to contours (Figure 6). The net rainfall becomes shallow subsurface flow, which is routed down flow tubes, allowing calculation of the local flux through each topographic element (Montgomery and Dietrich, 1994). Local wetness (*W*) is the ratio of the local flux at a given steady-state rainfall (*Q*) to that upon complete saturation of the soil profile:

$$W = \frac{Qa}{bT\sin\theta} \qquad (2)$$

where *a* is the upslope contributing area (m^2), *b* is the contour length across which flow is accounted for (m), *T* is the soil transmissivity (m^2/day), and θ is the local ground slope (degrees) (Montgomery et al., 2001). When wetness exceeds 1.0, we can adopt the simplified assumption that $W = h/z$ (Dietrich et al., 1995), where *h* is the thickness of the saturated soil above the impermeable layer and *z* is the total thickness of the soil (Montgomery et al., 2001). Combining this hydrologic model with the infinite-slope stability model provides a simple model for failure of shallow soils. The critical steady-state rainfall required to cause slope instability (Q_c) is given by:

$$Q_c = \frac{T\sin\theta}{(a/b)} + (\rho_s/\rho_w)[1-(\tan\theta/\tan\phi)] \qquad (3)$$

for cohesionless soils where ρ_s is the saturated bulk density of the soil, ρ_w is the density of water, ϕ is the friction angle of the soil, and *a*, *b*, *T* and θ are as stated for equation (2) (Montgomery et al., 2001; Montgomery and Dietrich, 1994). For soils with an apparent cohesion (C'), Q_c is given by equation (1) (Montgomery et al., 2001; Montgomery et al.,

1998). For this study the parameters were set to the following values to reasonably estimate general properties of glacial deposits (Montgomery et al., 2001; Koloshi et al., 1989): ($\rho s/\rho w$) = 2.0, C = 2, 4, and 8 kPa, ϕ = 33°, and T = 65 m^2/day (Montgomery et al., 2001).

Values of W greater than 1.0 implies excess water run off as overland flow, when W equals 1.0 the slope are unconditionally stable, and when W equal 0 the slopes are unconditionally unstable. Critical rainfall values of 0-50, 50-100, 100-200, 200-400, and greater than 400 mm/day can be calculated for slopes between these criteria (Montgomery et al., 2001).

WADNR Island County buildings database

To create the buildings database for Island County I used both Excel and ESRI ArcMap. Excel tables were used to organize and compile the information while ArcMap was used to further compile and spatially display it. This database contains parcel number with latitude and longitude direction, and building cost. The very first step was to compile the parcel records for every building in Island County. Some of the parcel records did not contain building cost and as a result, a web search was done from the Island County assessor website.

Determining landslide probability occurrence

The probability of occurrence was taken from Coe et al. (2000), where a probabilistic assessment was created for precipitation-triggered landslides in the City of Seattle. Coe et al. (2000) used ninety years of historical landslide records to input into Poisson and binomial probability models to calculate exceedance probability. In order to determine landslide probability occurrence for Island County I used different datasets consisting of: Freeland quadrangle SHALSTAB results, Seattle SHALSTAB results from Montgomery et al. (2001), and calculated exceedance probability from the Coe et al. (2000) study. First, I assigned landslide exceedance probability to each of the seven SHALSTAB classes (stable, unstable, greater than 400 mm/day, 200-400 mm/day, 100-200 mm/day, 50-100 mm/day, and 0-50 mm/day) by correlating the Seattle SHALSTAB results map

with the calculated exceedance probabilities map. The exceedance probability is mapped based on density (number of landslides per 4 hectare count circle) and is partially represented in Table 3 (see Appendix for whole table). Areas considered unstable by SHALSTAB fell mostly within a density of 10 landslides per 4 hectare count circle, which equals an exceedance probability of 10.5%. This same correlation procedure was applied to each SHALSTAB class (Table 4). Second step was to assign the Seattle SHALSTAB classes containing exceedance probabilities to the Freeland quadrangle SHALSTAB classes. Lastly, I divided the Freeland quadrangle into a 200 m x 200 m cell grid. The cell grids allowed me to aggregate the Freeland SHALSTAB results and obtain a mean critical rainfall per cell grid in order to assign an exceedance probability from Table 4.

Table 3. Seattle landslide densities, mean recurrence intervals, and probability (percent chance) of one or more landslides occurring during a specific time in the future

Density (number of landslides per 4 hectare count circle)	Mean Recurrence Interval (yrs)	1 yr. Exceedance Probability (percent chance of one or more landslides during a specific time)
1	88.40	1.12
2	40.20	2.24
3	29.47	3.34
4	22.10	4.42
5	17.68	5.50
6	14.73	6.56
7	12.63	7.61
8	11.05	8.65
9	9.82	9.86
10	8.84	10.70

Table 4. SHALSTAB results assigned to exceedance probability based on density

SHALSTAB results (mm/day)	Density (No. of landslides per 4 hectare count circle)	Exceedance Probability of 1 yr (percent chance of one or more landslides during a specified time)
Stable	-	-
> 400	2	2.2
200 – 400	2	2.2
100 – 200	2	2.2
50 – 100	2	2.2
0 - 50	6	6.5
Unstable	10	10.5

Risk assessment

In order to quantify risk for the field site, the following generic hazard-risk formula was used:

$$Risk = H \times (V \times A) \quad (4)$$

where *H* equals the hazard expressed as probability of occurrence within a reference period (in this study, 1 year), *V* equals physical vulnerability of a particular type of element at risk (from 0 to 1), and *A* equals the number or cost of the particular elements at risk (e.g., cost of buildings) (Van Weston, 2004).

Two shallow landslide scenarios were assessed in this study to determine property loss: (1) a minimum setback of 9 m and minimum runout of 60 m; and (2) a maximum setback of 12 m and maximum runout of 235 m. The runout distance was taken from the shallow landslide hazard map of Seattle study (Harp et al., 2008), and the setback distance for minimum and maximum bluff setback for residents was taken from the Department of Ecology Puget Sound landslides website. To determine which infrastructures would be affected, I digitized the bluff from the 3-foot hillshade LiDAR data using ArcMap. Then I created a buffer of the bluff for the two scenarios mentioned above. An overlay analysis of buffered polygons created based on scenario (1) and the WADNR Island

County structure location point database was done; the same was done for the buffered polygons created based on scenario (2). A grid of 200 m x 200 m cells was created for the study area (shown in Figure 7). This grid cell size was used because it is roughly equivalent in area to an average sized city lot (Coe et al., 2000). The minimum and maximum risk property loss were calculated for each cell containing structures that would be affected.

Assumptions and Limitations

Shallow landslide models

The biggest assumption and limitation made for this study was using shallow landslide models designed for mountainous hillslopes and applying them on a bluff environment. LRIM was primarily designed to identify Forest Practices rule-identified landforms (discussed in the Methods section) and thus might not be optimally applicable to an urbanized and bluff environment like Whidbey Island. LRIM takes into account only slope (percent rise) and curvature of the landscape to determine if areas are susceptible to shallow landslides. Other variables that might be important but that haven't been taken into account here are lithology, aspect, vegetation, wave undercutting, and bluff retreat. Table 4 shows the calibrations that were done for this project and the limitations met. A few experimental calibrations were also done to determine the limitations of the model.

Table 5. LRIM limitations based on calibrations made with varying percent slope and plan curvature

Calibrations	Percent Slope	Plan Curvature	Limitations of identified hazardous areas
WADNR	≥ 68	≤ -1	relatively precise
Island County	≥ 40	≤ -1	over estimated
Experiment 1	≥ 68	≤ -20	underestimated
Experiment 2	≥ 40	≤ -20	underestimated
Experiment 3	≥ 70	≤ -1	over estimated
Experiment 4	≥ 80	≤ -20	over estimated

SHALSTAB is limited by low-resolution digital topography, which results in incorrectly predicted stability (Dietrich et al., 1995). For the hydrologic model to map the spatial pattern of equilibrium soil saturation based on analysis of upslope contributing areas, soil transmissivity, and local slope, the model assumes that flow infiltrates to a lower conductivity layer and follows topographically-determined flow paths (Montgomery et al., 2001; O'Loughlin, 1986). The hydrologic model in SHALSTAB also assumes that the saturated conductivity does not vary with depth (Montgomery et al, 2001; Dietrich et al., 1995). Parameter variables such as soil properties and steady state precipitation vary spatially, but a single value is assigned to an entire landscape (Montgomery and Dietrich, 1994).

Landslide probability occurrence

One important assumption made in order to determine the landslide probability occurrence was that the exceedance probabilities determined for the Seattle area would be the same for Whidbey Island, which also meant assuming that all unstable areas contained an exceedance probability of 10.5. This was a reasonable assumption as the geologic setting of both Seattle and Whidbey Island are relatively the same and as a result, the landslide probability occurrence would be similar too. Also, in order to obtain the critical rainfall per city lot (200 m x 200 m cell grid), the SHALSTAB results had to be aggregated to a lower spatial resolution.

Areas at risk

To determine areas at risk, assumptions regarding the setback and runout for the two shallow landslide scenarios were made. The first assumption was that the minimum runout is 60 m and maximum runout is 235 m. This information was obtained as an average runout for shallow landslides of Seattle. The second assumption was that the minimum setback is 9 m and the maximum setback is 12 m established by the Department of Ecology. This information was not obtained from shallow landslide data but rather from the required setback a house should be from a bluff.

Results

Examining landslide geomorphic features

From LiDAR mapping and LRIM I was able to examine the geomorphic features that identified past instability and potential future instability. From LiDAR landform mapping, two major landslide complexes were identified (Figure 5). Both sites consisted of hummocky topography and evident headscarps. The first complex identified is just north of Lagoon Point, extending approximately 0.5 miles (Figure 5a). The second complex is south of Lagoon Point and north of Bush Point, extending approximately 2.0 miles (Figure 5c). A third landslide complex was identified by WADNR 24 k geologic mapping located just south of the first complex in Lagoon Point (Figure 5b). Although there is no evidence of current landsliding within these three areas, geologic mapping conducted by WADNR identified Quaternary mass-wasting deposits (Qls), suggesting evidence of failure in the past.

LRIM hazardous areas

The LRIM predictions using the WADNR forest practice standard thresholds (Table 1) suggested that the majority of the westerly slopes consist of hazardous areas (Figure 8). When observing the three landslide complexes they exhibit hazardous areas mainly along the headscarp and the toe (Figure 8a, b, c). LRIM output using the Island County thresholds (Table 1) estimates even more hazardous areas, indicating that the slopes along the bluff are at 40 degrees or greater. Figure 9 shows a comparison between the WADNR forest practice thresholds and the Island County thresholds for the three landslide complexes. The Island County thresholds identify more hazardous areas within each landslide complex indicating that there are slopes greater or equal to 40 percent. Overall the WADNR threshold identifies steeper slopes at greater or equal to 68 percent that would be considered more hazardous over slopes at greater or equal to 40 percent. As a result, the WADNR forest practice standard thresholds will be considered for this study to identifying hazardous areas.

SHALSTAB unstable slopes

The results obtained from SHALSTAB show that the bluffs are unstable, but that the instability and hence probability of failure depends on the amount of rainfall. Figure 10 shows that the slopes are averaged as unconditionally unstable (light yellow), but contain small areas that will be unstable at a given critical rainfall. For instance, the more northern landslide complex contains about 20,000 m^2 with an average critical rainfall of 100-200 mm/day, 40,000 m^2 with 200-400 mm/day, and 20,000 m^2 with unconditionally unstable slopes (Figure 10a). The middle landslide complex contains about 20,000 m^2 with unconditionally unstable slopes, 120,000 m^2 with an average critical rainfall of 0-50 mm/day, and 40,000 m^2 with 50-100 mm/day (Figure 10b). The southern landslide complex contains about 40,000 m^2 with an average critical rainfall of 50-100 mm/day, 180,000 m^2 with unconditionally unstable slopes, and 40,000 m^2 with 0-50 mm/day (Figure 10c).

Risk

This data is expressed per 200 m x 200 m cell grid and determined for both minimum shallow landslide (setback of 9 m, runout of 60 m) and maximum shallow landslide (setback of 12 m, runout of 235 m) scenarios. The risk equation (equation 4) was applied to each 200 m x 200 m cell grid because each grid contained varying *H* variable (hazard expressed as probability of occurrence within a reference period, 1 year), and *A* variable (number or cost of the particular elements at risk, cost of buildings) (Table 6). For the minimum landslide scenario a total of 27 cell grids were totaled to obtain a minimum risk calculation. This scenario resulted in a total damage of 57 building, total property cost of $8,000,000, and risk of 31,000,000 U.S dollars/1 year. For the maximum landslide scenario a total of 41 cell grids were totaled to obtain a maximum risk calculation. This scenario resulted in a total damage of 203 building, total property cost of $32,600,000, and risk of 130,000,000 U.S dollars/1 year. Figures 11a and 11b identify the location of the 57 buildings that would be affected by a minimum landslide event. Figures 12a and 12b identify the location of the 203 buildings that would be affected by a maximum landslide event.

Table 6: Risk values used to calculate risk assessment for both minimum and maximum shallow landslide scenarios

Point	Vulnerability	Min. Value (U.S dollars)	Max. Value (U.S dollars)	Min. Count (buildings)	Max. Count (buildings)	Exceedance Probability of 1 yr (% chance of one or more landslides during a specified time)	Min. Risk (U.S dollars/1 yr)	Max. Risk (U.S dollars/1 yr)
1	1	155467	155467	3	3	10.5	1632403.5	1632403.5
2	1	233307	233307	1	1	2.2	513275.4	513275.4
3	1	0	113488	0	1	2.2	0	249673.6
4	1	0	476598	0	2	6.5	0	3097887
5	1	19258	262384	1	5	6.5	125177	1705496
6	1	140341	1740944	1	18	6.5	0	11316136
7	1	0	96524	0	2	6.5	0	627406
8	1	126454	496882	1	11	6.5	821951	3229733
9	1	891649	1998266	8	13	2.2	1961627.8	4396185.2
10	1	1045446	2359440	11	19	6.5	6795399	15336360
11	1	40000	1818779	1	14	2.2	88000	4001313.8
12	1	0	897678	0	7	2.2	0	1974891.6
13	1	98112	559862	1	3	10.5	1030176	5878551
14	1	307899	2819814	3	7	2.2	677377.8	6203590.8
15	1	222342	511983	4	5	2.2	489152.4	1126362.6
16	1	232604	756889	1	3	10.5	2442342	7947334.5
17	1	155613	497304	1	3	10.5	1633936.5	5221692
18	1	248908	248908	1	1	6.5	1617902	1617902
19	1	109282	387826	1	2	2.2	240420.4	853217.2
20	1	118530	118530	1	1	10.5	1244565	1244565
21	1	188954	188954	1	1	2.2	415698.8	415698.8
22	1	112804	319986	1	2	6.5	733226	2079909
23	1	684376	986006	3	4	2.2	1505627.2	2169213.2
24	1	0	526147	0	1	2.2	0	1157523.4
25	1	218250	893113	1	3	6.5	1418625	5805234.5
26	1	127591	127591	1	1	6.5	829341.5	829341.5
27	1	0	230644	0	1	6.5	0	1499186
28	1	62464	62464	1	1	2.2	137420.8	137420.8
29	1	234076	1555523	1	4	2.2	514967.2	3422150.6
30	1	484635	961797	1	5	2.2	1066197	2115953.4
31	1	0	292823	0	1	2.2	0	644210.6
32	1	140309	1683000	1	2	2.2	308679.6	3702600
33	1	700832	700832	2	2	2.2	1541830.4	1541830.4
34	1	54097	236225	1	2	2.2	119013.4	519695
35	1	359174	1015409	3	6	2.2	790182.8	2233899.8
36	1	0	1645514	0	19	6.5	0	10695841
37	1	0	979729	0	5	2.2	0	2155403.8
38	1	0	1391116	0	10	6.5	0	9042254
39	1	0	831063	0	6	2.2	0	1828338.6
40	1	0	1216259	0	5	2.2	0	2675769.8
41	1	0	195478	0	1	2.2	0	430051
Total	**-**	**8000000**	**32600000**	**57**	**203**	**-**	**30694515.7**	**133275502**

Discussion

Identifying unstable slopes using shallow landslide models

LiDAR mapping and geologic mapping identified three landslide complexes along the bluffs of the 7.5 minute Freeland quadrangle. Since there is no evidence of recent sliding, LRIM and SHALSTAB were used to identify potential instability within the three landslide complexes. LRIM was used to identify hazardous areas and SHALSTAB was used to further determine the instability based on critical rainfall (mm/day). For the first (northern) landslide complex, LRIM identified hazardous areas mainly along the headscarp and toe (Figure 8a). The SHALSTAB results identified these same areas as unconditionally unstable (Figure 10a). For the second (middle) landslide complex LRIM identified hazardous areas along the majority of the slope (Figure 8b). The SHALSTAB results identified the headscarp as unconditionally unstable and with the rest of the bluff ranging from 0-50 mm/day, 50-100 mm/day, and 100-200 mm/day (Figure 10b). And for the third (southern) landslide complex LRIM also identified hazardous areas along the headscarp and toe of the complex (Figure 8c). The SHALSTAB results then also identified these same areas as unconditionally unstable (Figure 10c). Based on these results, both LRIM and SHALSTAB identify the same unstable areas. However, the SHALSTAB results take more parameters into account for instance, cohesion, bulk density, water density, and friction angle. With all these parameters accounted for SHALSTAB is able to provide the critical rainfall required to cause slope instability while LRIM just provides areas of potential hazard based on specified thresholds.

For this study, SHALSTAB was also helpful in assigning landslide exceedance probability for the 7.5-minute Freeland quadrangle. Unlike the study conducted for the City of Seattle by Coe et al., (2000), which allowed them to calculate exceedance probabilities using historic landslide records, Island County contains no such information. Further studies like the one conducted in Seattle should be done on Island County by examining old landslide complexes to determine exceedance probabilities. Such a study would further aid this risk assessment and future landslide studies.

Risk assessment

The shallow landslide scenarios indicate that a total of 203 buildings could be affected by future slope failures, a number of which are located outside of the previously identified landslide complexes. The total property loss is estimated at approximately $32,600,000. Figure 12 shows the location of each building that would be affected by the maximum shallow landslide with a setback of 12 m and a runout of 235 m. These include buildings that are above the slope and would be affected by the setback of the land and buildings below the slope that would be affect by the runout. The residents living along either of the three landslide complexes should be advised of potential sliding. The second landslide complex in particular shows a large amount of buildings being affected by a maximum runout (Figure 12). Although many residents outside of the three complexes are also in potential danger of a landslide, as previously mentioned, some bluffs have not yet failed but have the potential of failing and affecting more residents.

Island County's coastal areas are vulnerable to landslides and the results from the shallow landslide risk assessment of the Freeland quadrangle are a good example. Currently, ordinances identifying geological hazards are in effect and information regarding steep slope hazards is available from county and city planning and building departments. Where the established ordinances are rigorously applied landslide losses are reduced by 95-100 percent (Island County, 2006). According to Island County's Multi-jurisdiction Hazard Mitigation Plan (2006) the least expensive and most effective landslide loss reduction measure is avoidance followed by mitigation using qualified expertise with an investigation report review process. The most costly expense of landslides is repair of damages. Overall the cost of proper mitigation is approximately one percent of the costs otherwise incurred through losses and litigation (Island County, 2006).

Island County Department of Emergency Management (DEM) is currently working with the Washington State Emergency Management Division (EMD) and the State Homeland Security Region 1 on updating its Hazard Mitigation Plan. DEM is responsible for emergency planning including planning and coordination actions for the preparedness, mitigation, response, and recovery form natural and man-made emergencies and disasters

(Island County Emergency Management, http://www.islandcountydem.org/hazard-mitigation-plan.html). The Hazard Mitigation Plan will consist of a document and hazard maps, but currently no drafts are available for viewing.

Conclusion

Geomorphic analysis of landslide features revealed that the westerly bluffs of the Freeland quadrangle have experienced landsliding in the past. Two landslide complexes consisting of hummocky topography, benches, and prominent headscarps were identified using LiDAR. One landslide complex was identified based on Quaternary mass-wasting deposits (Qls) conducted by WADNR geologic mapping. Results from LRIM and SHALSTAB GIS modeling support assessments that suggest that hazardous and unstable bluffs occur within the two complexes and all along the westerly bluffs.

The risk assessment highlighted the potential for property damage in the event of scenarios of two shallow landslide scenarios: (1) a minimum setback of 9 m and minimum runout of 60 m and (2) a maximum setback of 12 m and maximum runout of 235 m. A landslide risk equation by Van Westen (2004) was used to calculate risk and determine estimated property loss for each scenario. The estimated total property loss calculated for the first shallow landslide scenario was approximately $8,000,000 affected 57 buildings. On the other hand, the estimated total property loss calculated for the second shallow landslide scenario was approximately $32,600,000 affecting 203 buildings. Although a major assumption was made to calculate the risk by taking the recurrence interval determined for the City of Seattle and applying it to Whidbey Island, the approach nevertheless provided a general estimate of the potential risks at hand. In conclusion, further studies of old landslide complexes on Whidbey Island should be studied in order to establish a landslide recurrence interval for the area and to further improve this risk assessment.

References

Booth, D. B., 1994. Glaciofluvial infilling and scour of the Puget Lowland, Washington, during ice-sheet glaciation. *Geology* 22, 695 – 698.

Booth, D. B., Troost, K. G., and Clague, J. J., 2003. The Cordilleran Ice Sheet. *Developments in Quaternary Sciences* 1, 17 – 43.

Booth, D. B., Troost, K. G., and Hagstrum, J. T., 2004. Deformation of Quaternary strata and its relationship to crustal folds and faults, south-central Puget Lowland, Washington State. *Geology* 32, 505 – 508.

Coe, J. A., Michael, J. A., Crovelli, R. A., and Savage, W. Z., 2000. Preliminary map showing landslide densities, mean recurrence intervals, and exceedance probabilities as determined from historic records, Seattle, Washington. *U.S Geological Survey Open File Report 00-303, paper edition*.

Cruden, D. M., 1991. A simple definition of a landslide. *Bulletin of the International Association of Engineering Geology* 43, 27 – 29.

Department of Ecology https://fortress.wa.gov/ecy/coastalatlas/tools/Map.aspx

Dietrich, W. E., Reiss, R., Hsu, M. L., and Montgomery, D. R., 1995. A process-based model for colluvial soil depth and shallow landsliding using digital elevation data. *Hydrological Processes* 9, 383 – 400.

Easterbrook, D. J., Crandell, D. R., and Leopold, E. B., 1967. Pre-Olympia Pleistocene stratigraphy and chronology in the central Puget Lowland, Washington. *Geological Society of America, Bulletin* 78, 13 – 20.

Finn, C., Phillip, W. M., and Williams, D. L., 1991. Gravity anomaly and terrain maps of Washington. *U.S. Geological Survey Geophysical Investigations Map* GP-988, scale 1:100,000 and 1:500,000.

Finn, C., 1995. Preliminary merged aeromagnetic map of north-western Washington. *U.S. Geological Survey Open-File Report* 95-212, scale 1:250,000.

Geotechnical Engineering Services, 2013. Ledgewood Landslide Evaluation Whidbey Island, Washington. File No. 0422-097-00.

Geotechnical Extreme Events Reconnaissance, 2014. The 22 March 2014 Oso Landslide, Snohomish County, Washington.

Gower, H. D., Yount, J. C., and Crosson, R. S., 1985. Seismotectonic map of the Puget Sound region, Washington. *U.S Geological Survey Map* I-1613, scale 1:250,000.

Harp E. L., Michael, J. A., and Laprada, W. T., 2008. Shallow landslide hazard map of Seattle, Washington. *Engineering Geology XX*, 67 – 82.

Highland, L., 2004. Landslide types and processes. *U.S. Geological Survey* 2004-3072.

Island County, 2006. Island County Multi-Jurisdiction Hazard Mitigation Appendix B. https://www.islandcounty.net/publicworks/DEM/documents/AppendixBV4.pdf.

Island County, Washington-Code of Ordinances, 2015. Land Development Standards. Ordinance No. HD-07-15.

Island County Emergency Management. Island County Department of Emergency Management. http://www.islandcountydem.org/hazard-mitigation-plan.html

Johnson, S. Y., Potter, C. J., and Armentrout, J.M., 1994. Origin and evolution of the Seattle fault and Seattle basin, Washington. *Geology* 22, 71 – 74.

Johnson, S. Y., Potter, C. J., and Armentrout, J. M., Miller, J. J., Finn, C., and Weaver, C. S., 1996. The southern Whidbey Island fault: An active structure in the Puget Lowland, Washington. *GSA Bulletin* 108, 334 – 354.

Koloshi, J. W., Schwarts, S. D., and Tubbs, D. W., 1989. Geotechnical properties of geologic materials. *Washington Division of Geology and Earth Resources Bulletin* 78, 19 – 26.

Mullineaux, D. R., Waldron, H. H., and Rubin, M. (1965). Stratigraphy and chronology of late interglacial and early Vashon time in the Seattle area, Washington. *U.S. Geological Survey Bulletin* 1194-0. 01 – 010.

Montgomery, D. R., and Dietrich, W. E., 1994. A physically based model for the topographic control on shallow landsliding. *Water Resources Research* 30, 1153 – 1171.

Montgomery, D. R., Sullivan, K., Greenberg, H. M., and Dietrich, W. E., 2000. Forest clearing and regional test of a model for shallow landsliding. *Hydrological Processes* 28, 311 – 314.

Montgomery, D. R., Greenberg, H. M., Laprade W. T., and Nashem, W., D., 2001. Sliding in Seattle: test of a model of shallow landsliding potential in an urban environment. *American Geophysical Union* 2, 59 – 73.

O'Loughlin, E. M., 1986. Prediction of surface saturation zones in natural catchments by topographic analysis. *Water Resources Research* 22, 794 – 804.

PSLC, 2015. 2000-2005 Lower Puget Sound Projects. www.pugetsoundlidar.org

Porter, S. C. and Swanson, T. W., 1998. Radiocarbon age constraints on rates of advance and retreat of the Puget lobe of the Cordilleran ice sheet during the last glaciation. *Quaternary Research* 50, 205 – 213.

Schulz, H. W., 2007. Landslide susceptibility revealed by LIDAR imagery and historic records, Seattle, Washington. *Engineering Geology* 89, 67 – 87.

Schuster, R. L., 1996. Socioeconomic significance of landslides. In: Turner, A. K., Schuster, R. L. (Eds.), Landslides: Investigation and Mitigation, special report 247, Transportation Research Council, 12 – 35.

Schuster, R. L. and Leighton, R. W., 1988. Socioeconomic significance of landslides and mudflows. *UNESCO/UNEP*, 131 – 141.

Sedar, C. F., 2007. Recognition of non-rule identified high hazard landforms identified during landslide hazard zonation project mapping in Washington State. Geological Society of America Cordilleran section – 103rd Annual Meeting.

Shipman, H., 2001. Coastal landsliding on Puget Sound – a review of landslides occurring between 1996 and 1999. *Washington Department of Ecology, Shorelands and Environmental Assistance Program* 01-06-019.

Shipman, Hugh, 2004. Coastal bluffs and sea cliffs on Puget Sound, Washington. *U.S. Geological Survey Professional Paper* 1693, 81 – 95.

Slaughter S., Sarikhan, I., Polenz, M., and Walsh, T., 2013. Quick report of the Ledgewood-Bonair Landslide, Whidbey Island, Island County, Washington. Department of Natural Resources, Division of Geology and Earth Resources.

Slosson, J. E., and Krohn, J. P., 1982. Southern California landslides of 1978 and 1980. Storms, floods, and debris flows in southern California and Arizona, 1978 and 1980. Proceedings of a Symposium, National Research Council, and Environmental Quality Laboratory, California Institute of Technology, Pasadena, CA, 17 – 18 September 1980. *National Academy Press*, 291 – 319.

Swanson, T. W., Late Pleistocene glacial history of Whidbey Island, WA. http://faculty.washington.edu/tswanson/009302add/Field%20Trips/Trip2

Technical University of Catalonia, 2011. Guidelines for landslide susceptibility, hazard and risk zoning. Grant Agreement No.:226479.

Troost, K. G., Booth, D. B., 2008. Geology of Seattle and the Seattle area, Washington. *Geological Society of America Reviews in Engineering Geology XX*, 1 – 35.

U.S Geological Survey, 2015. Landslides Hazards of Seattle, WA, and vicinity. http://landslides.usgs.gov/state_local/seattle.php

Van Westen, C. J., 2004. Geo-Information tools for landslide risk assessment: an overview of recent developments. *Landslide: Evaluation and Stabilization, Lacerda, Ehrlich, Fontoura & Sayã0 (eds),* ISBN 04 1535 665 2.

Vance-Sherman, A., 2014. Island County Profile. https://fortress.wa.gov/esd/employmentdata/reports-publications/regional-reports/county-profiles/island-county-profile

Washington State Department of Natural Resources, 2010. Landform Remote Identification Model (LRIM) Tool. Earth Sciences Program for State Trust Lands.

Washington Division of Geology and Earth Resources, 2014. Washington State landslides and landforms--GIS data, December, 2014: *Washington Division of Geology and Earth Resources Digital Data Series* DS-12, version 2.0.

Washington Division of Geology and Earth Resources. Landslides. http://www.dnr.wa.gov/ResearchScience/Topics/GeologicHazardsMapping/Pages/landslides.aspx).

Wells, R. E., Weaver, C. S., and Blakely, R. J., 1998. Fore-arc migration in Cascadia and its neotectonic significance. *Geology* 26, 759 – 762.

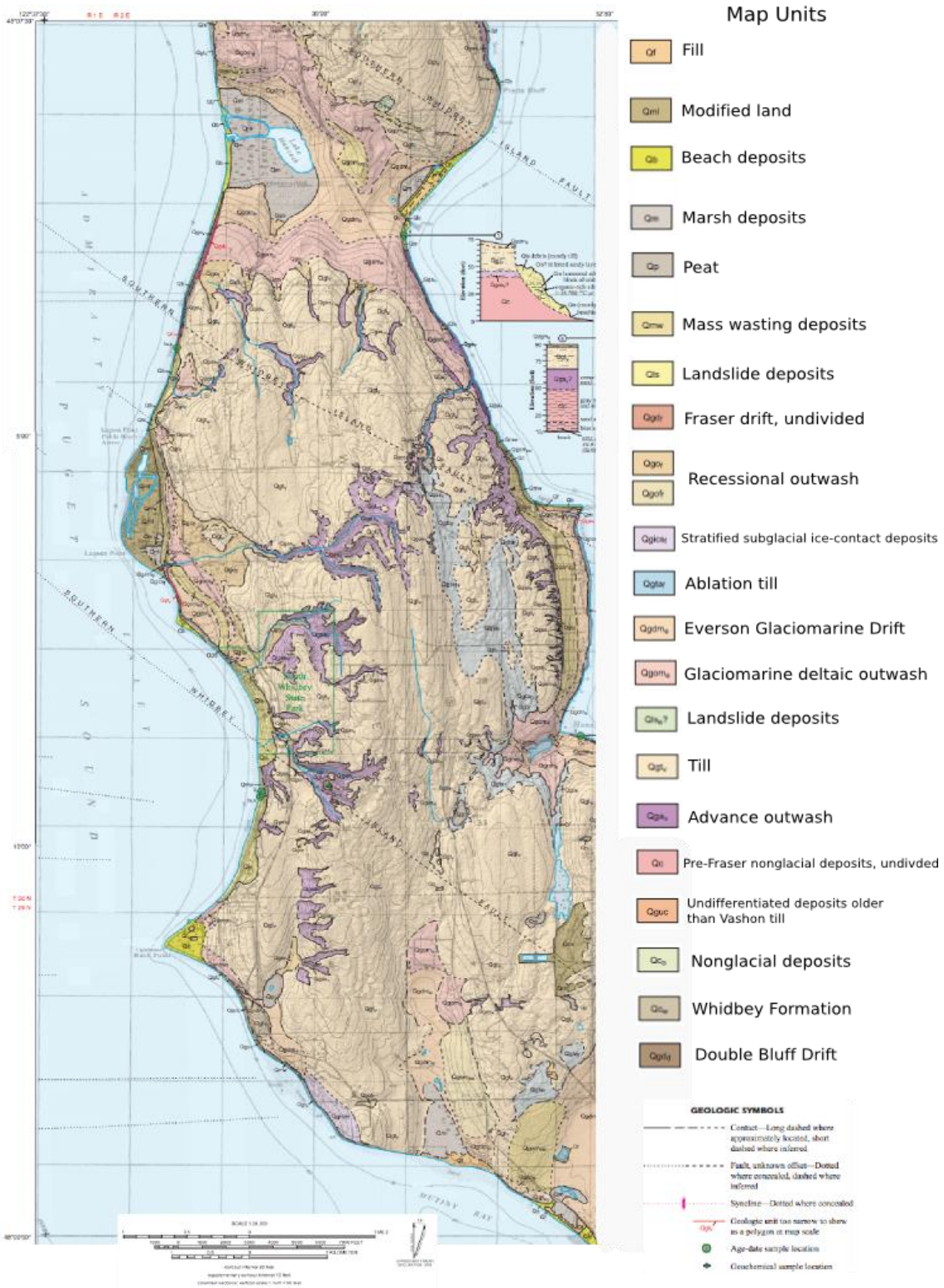

Figure 1. Geologic map of 7.5-minute Freeland Quadrangle, Island County, Washington from Washington Department of Natural Resources. (Modified by Evelyn Conrado, 2015)

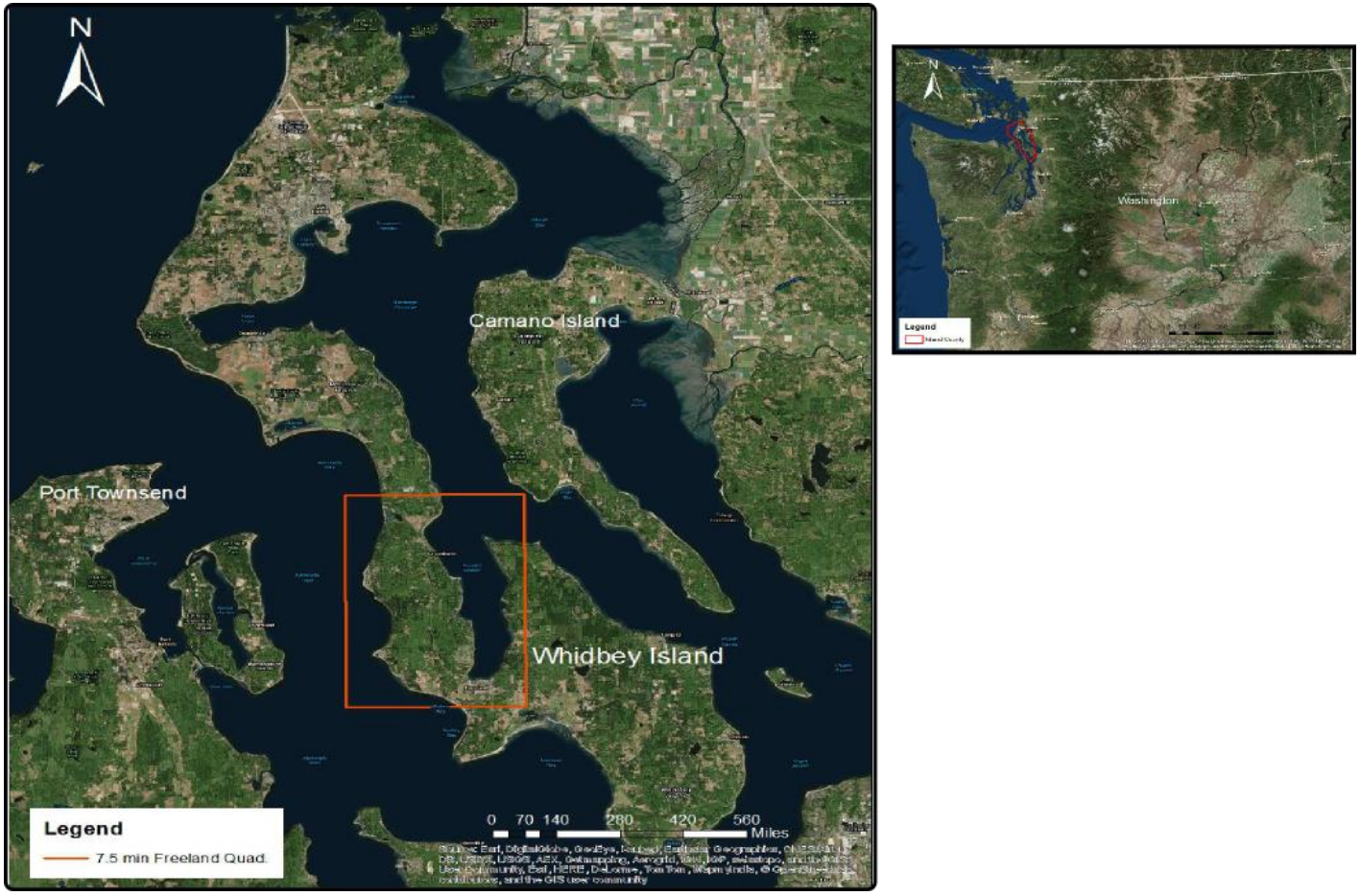

Figure 2. Location of Island County, WA in red (right) and location of 7.5 minute Freeland Quadrangle, Whidbey Island in orange (left).

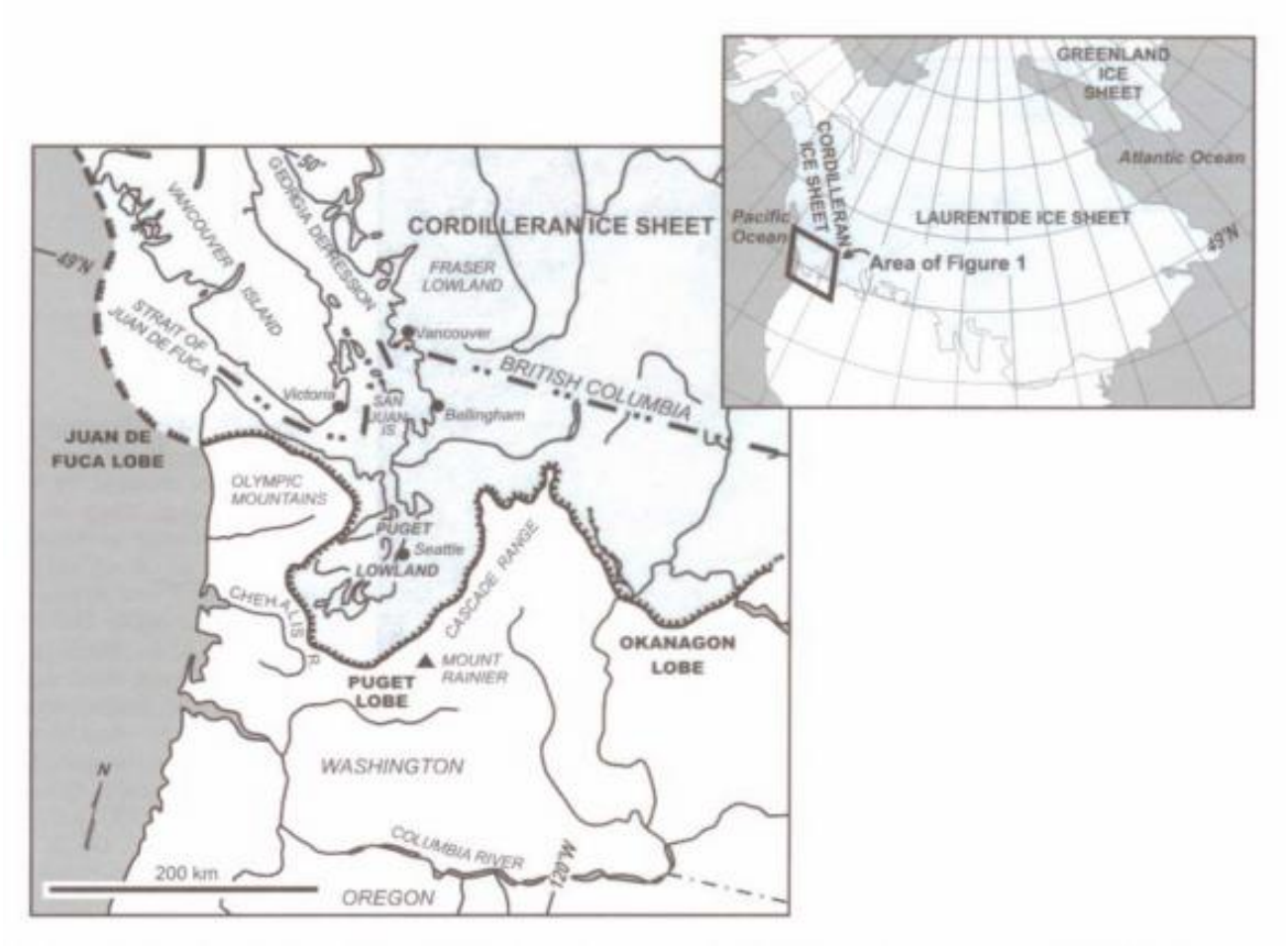

Figure 3. Location and extent of the Puget Lobe (shown by hachure marks) in Washington State (modified from Booth et al., 2004b) (source Troost and Booth, 2008)

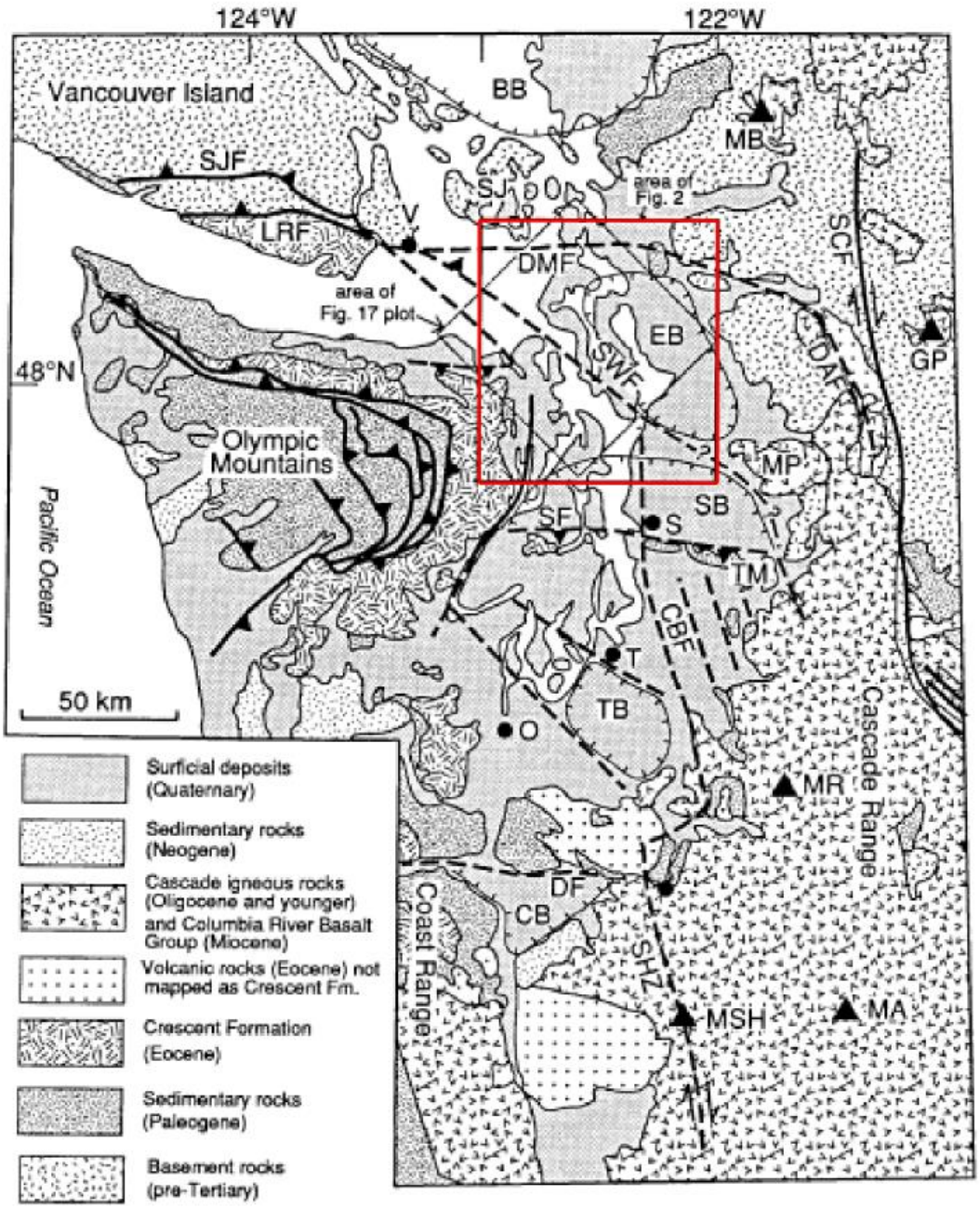

Figure 4. The northwest-trending southern Whidbey Island fault (SWIF) indicated by red box (source Johnson et. al., 1996)

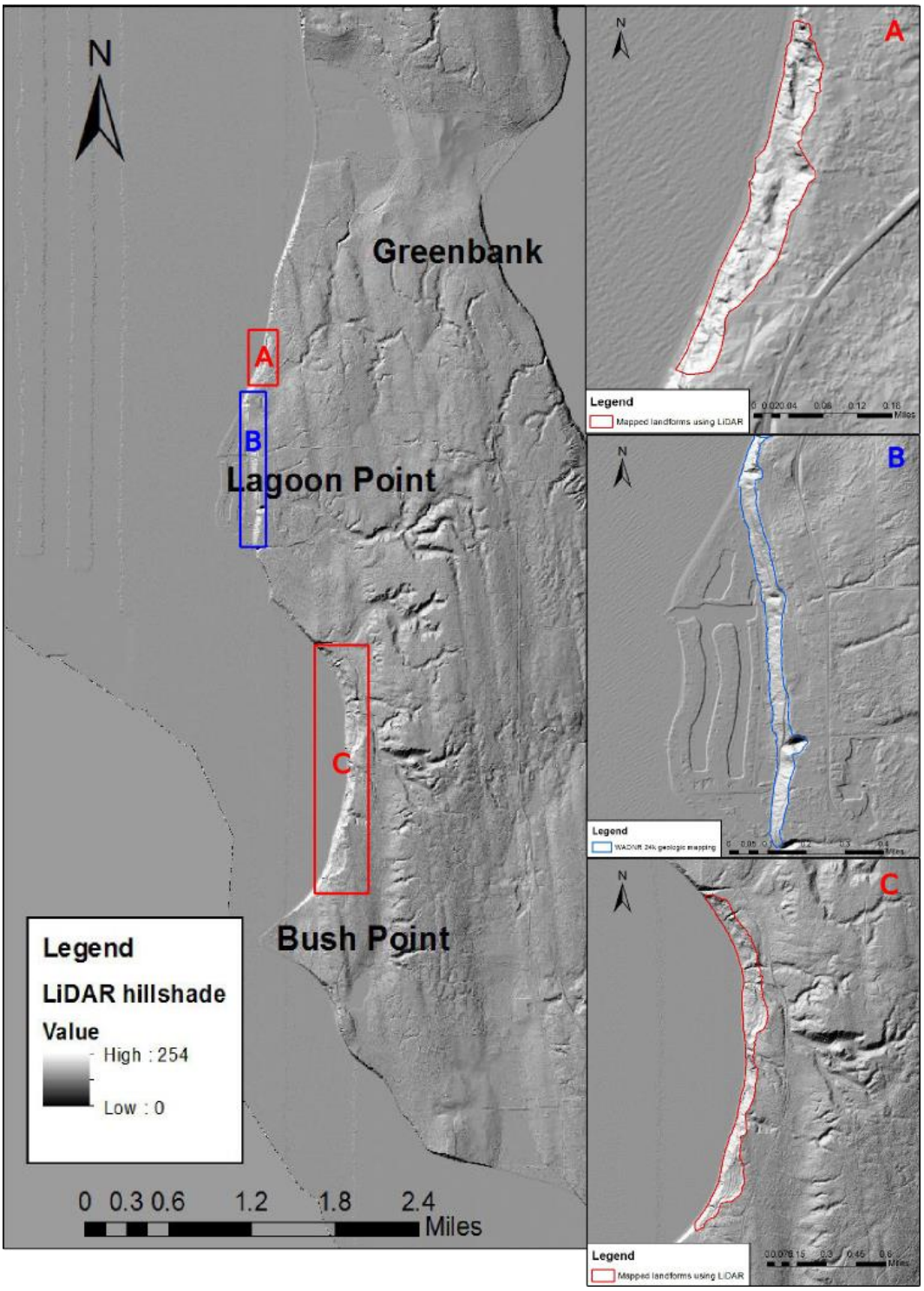

Figure 5. Mapped landforms using 6-foot hillshade LiDAR identified in red in box A and C (right). Mapped landform identified by WADNR identified in blue in box B (right). Map on the left shows the 7.5-minute Freeland Quadrangle and where each landform is located relative to Lagoon Point, Bush Point, and Greenbank.

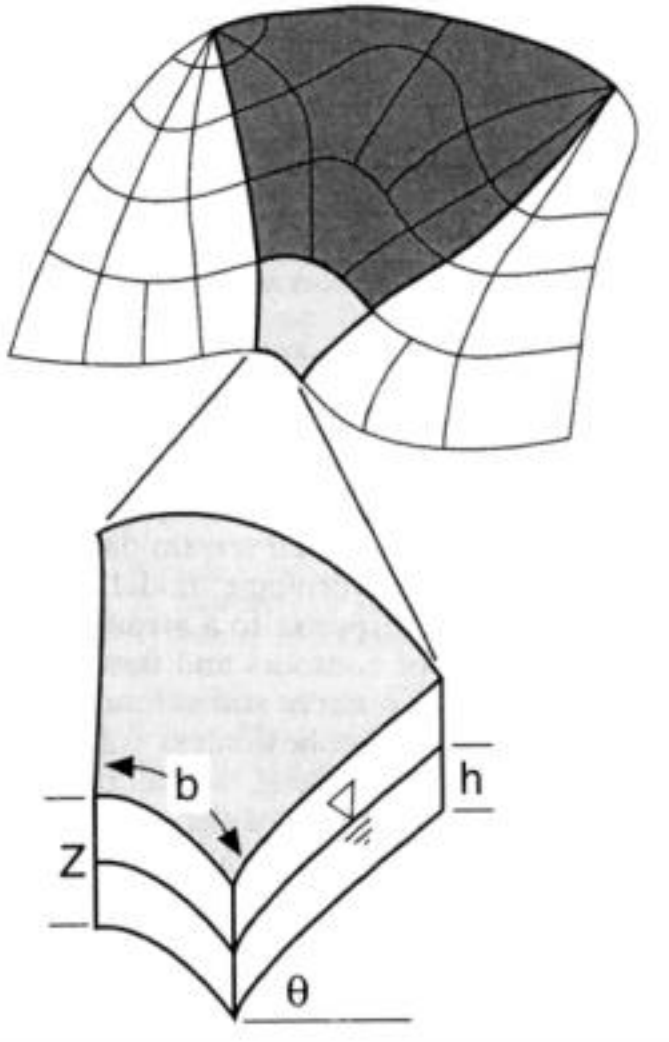

Figure 6. Intersections of contours (gray lines) and flow tube boundaries (black lines). Z equals total soil thickness, h equals thickness of saturated soil, b equals contour length of the lower bound to each element, and θ equals local slope (in degrees) of the ground surface. (Source Montgomery and Dietrich, 1994).

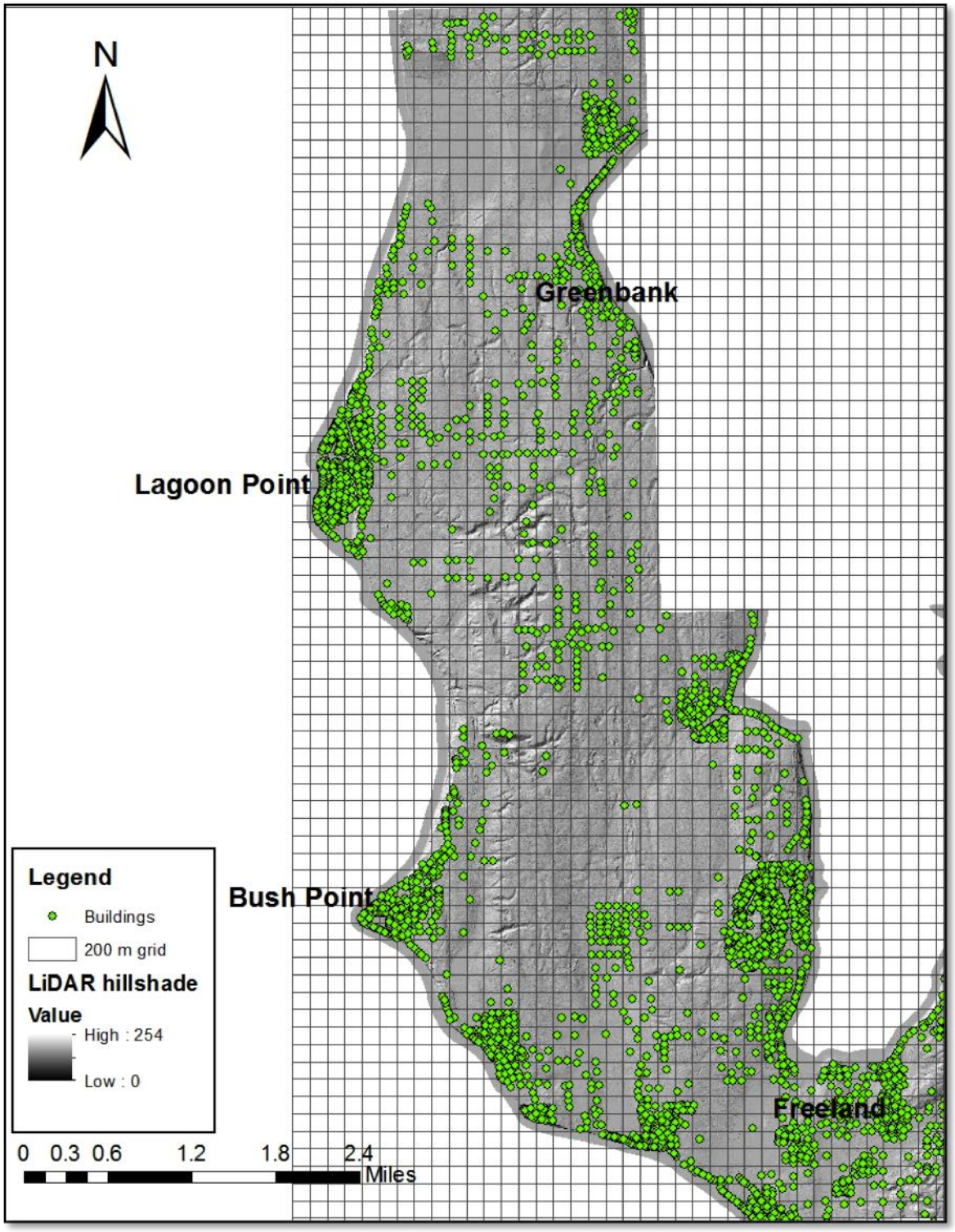

Figure 7. 7.5-minute Freeland quadrangle indicating where each building is located (green points) in a 200 m x 200 m cell grid.

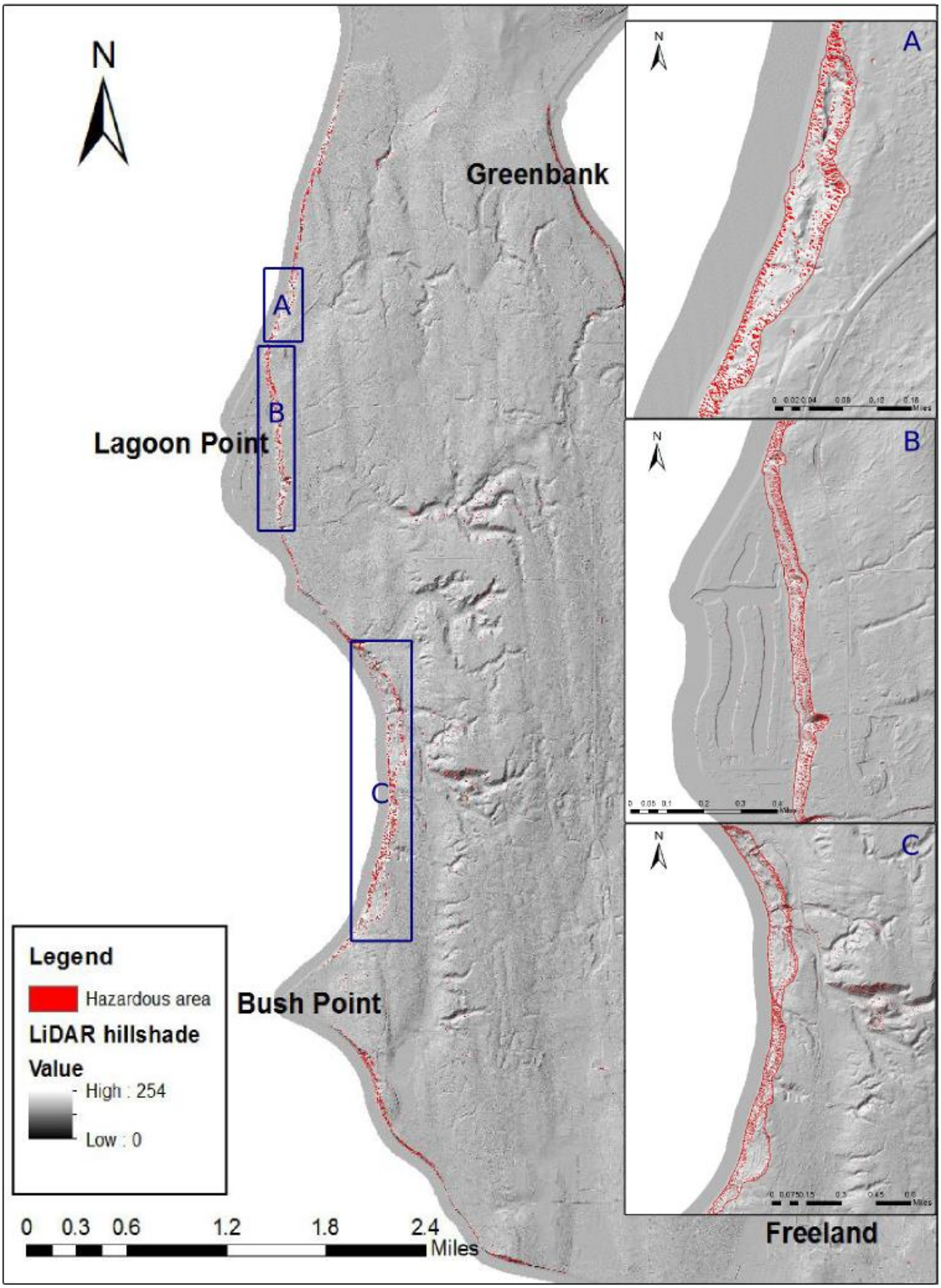

Figure 8. Landform Remote Identification Model (LRIM) WADNR calibration results (red), using thresholds of slope percent greater or equal to 68 and plan curvature less than or equal to -1. Box A (right) is zoomed into the northern landslide mapped in Figure 5. Box B (right) is zoomed into the middle landslide also mapped in Figure 5. Box C (right) is zoomed into the southern landslide mapped in Figure 5. Map on the right shows overall LRIM results for the whole quadrangle and location of each mapped landslide relative to Lagoon Point, Bush Point, Greenbank, and Freeland.

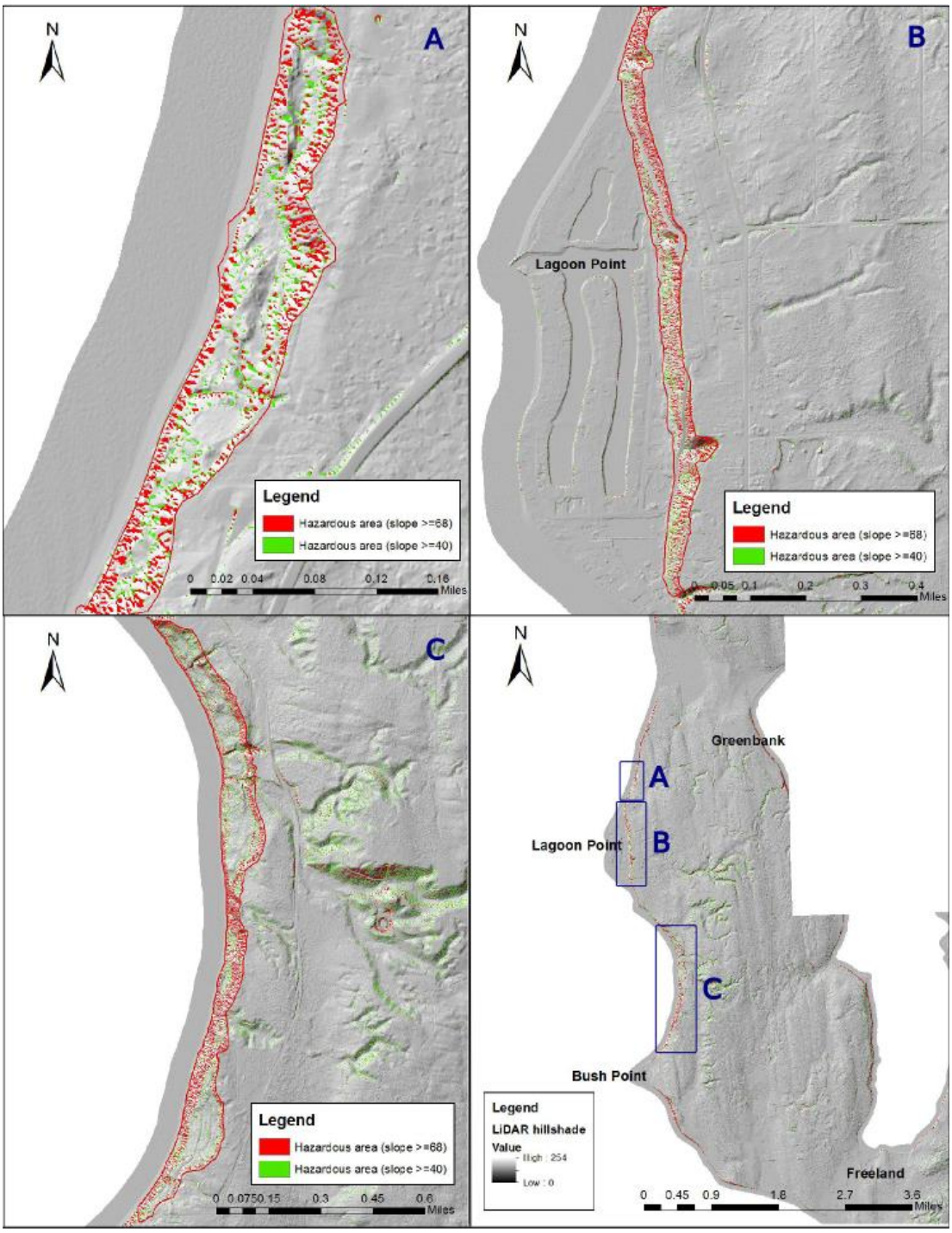

Figure 9. Landform Remote Identification Model (LRIM) comparison between the WADNR (red) and the Island County thresholds (green) on northern (a), middle (b), and southern (c) landslide complex. Map on bottom right indicates their location (blue boxes) relative to Lagoon Point, Bush Point, Greenbank, and Freeland.

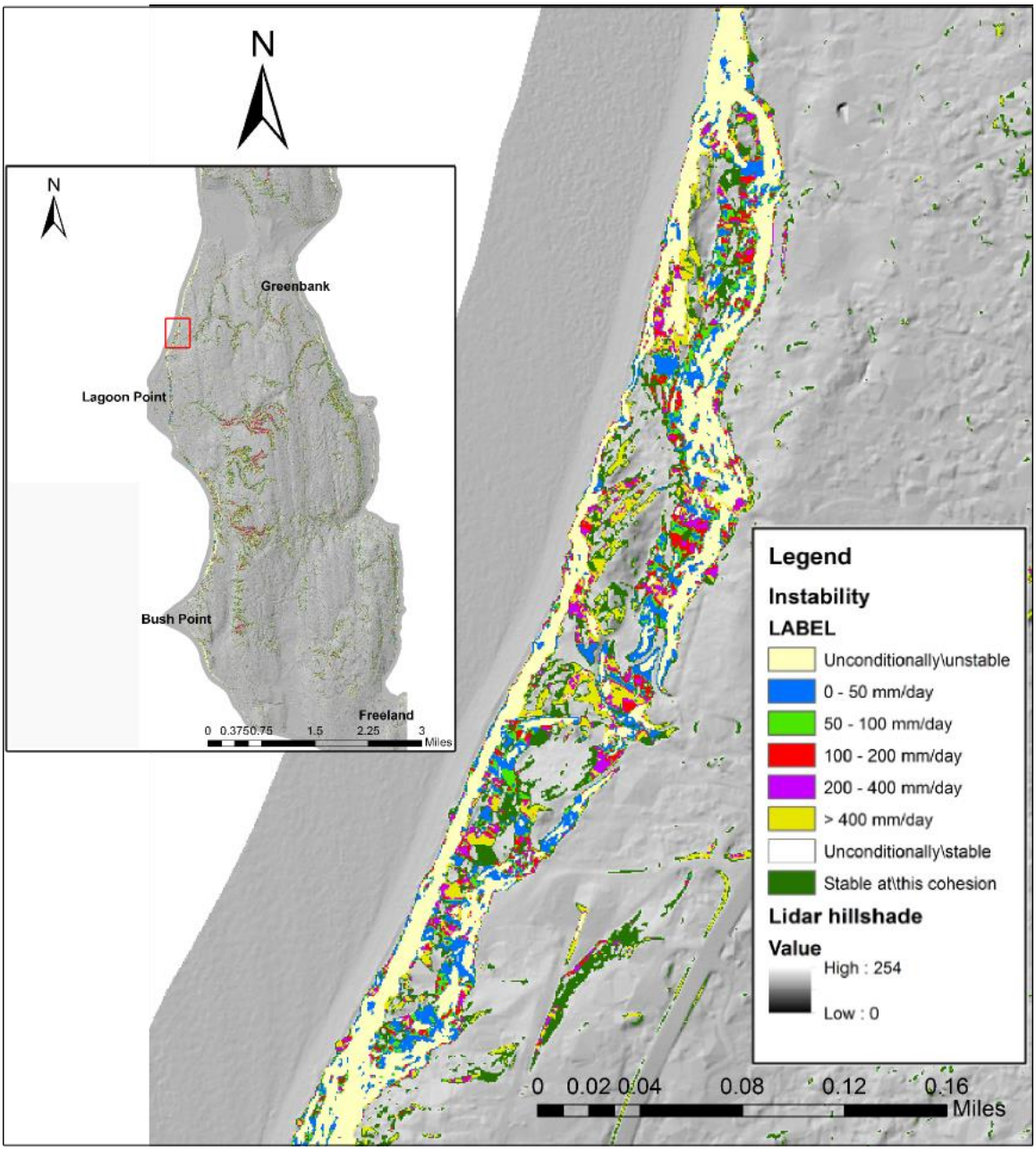

Figure 10a. Shallow Slope Stability Model (SHALSTAB) results identifying stability of slopes based on critical rainfall of the northern landslide complex. Map on the left identifies the location of the northern landslide complex (red box) relative to Lagoon Point, Bush Point, Greenbank, and Freeland.

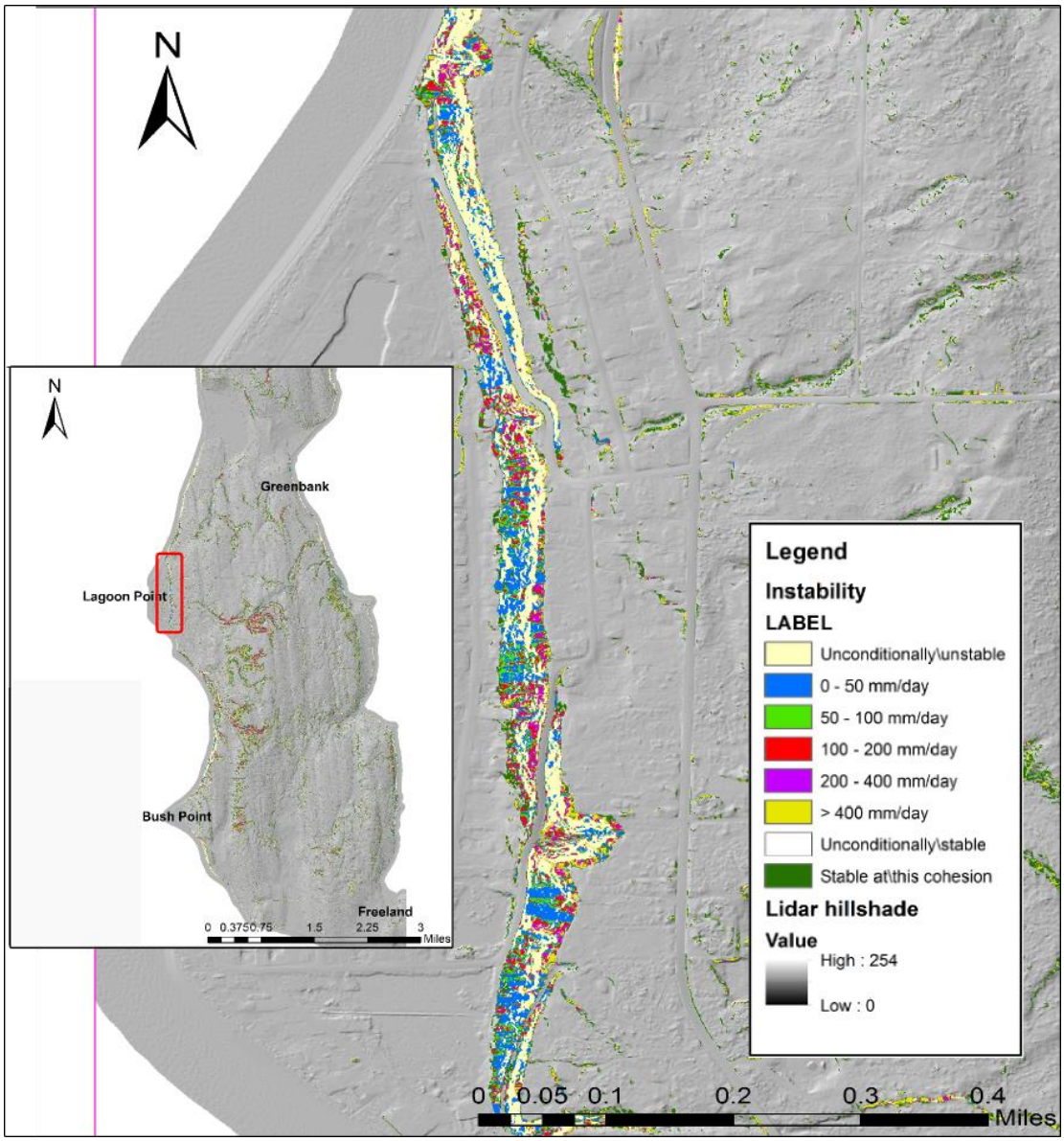

Figure 10b. Shallow Slope Stability Model (SHALSTAB) results identifying stability of slopes based on critical rainfall of the middle landslide complex. Map on the left identifies the location of the middle landslide complex (red box) relative to Lagoon Point, Bush Point, Greenbank, and Freeland.

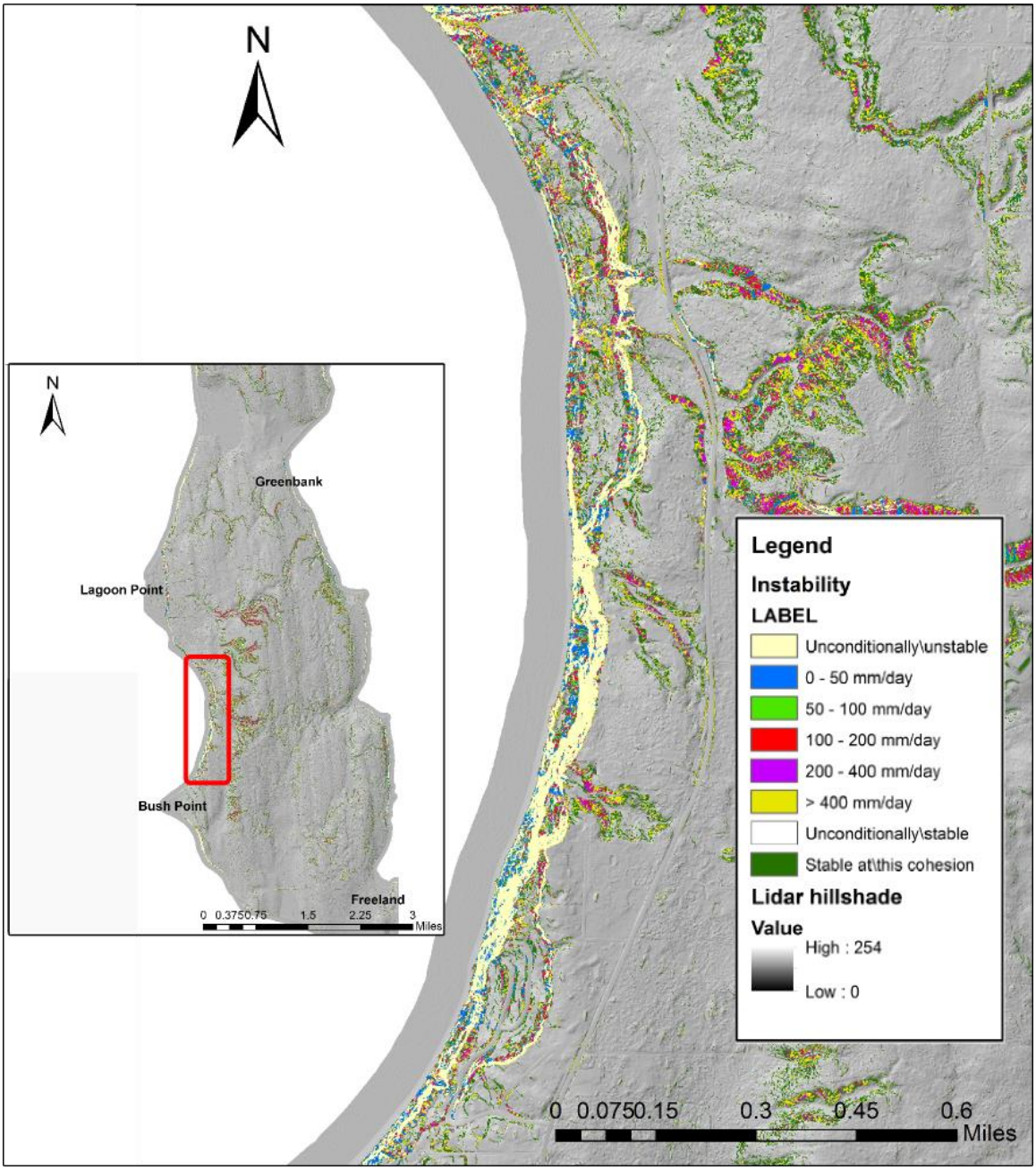

Figure 10c. Shallow Slope Stability Model (SHALSTAB) results identifying stability of slopes based on critical rainfall of the southern landslide complex. Map on the left identifies the location of the southern landslide complex (red box) relative to Lagoon Point, Bush Point, Greenbank, and Freeland.

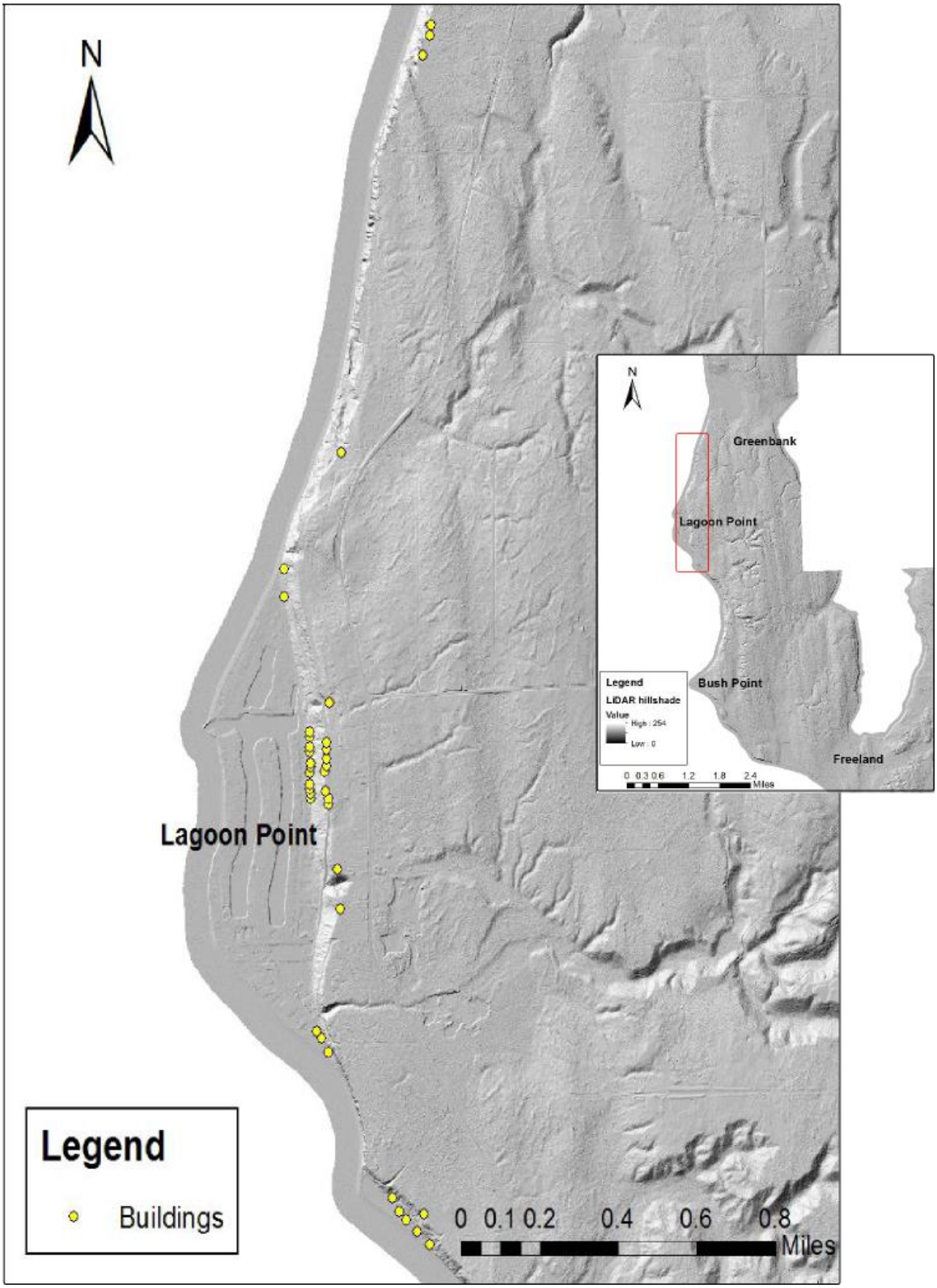

Figure 11a. Buildings (yellow points) that would be affected from a shallow landslide with a setback of 9 m and a runout of 60 m. Map on the left indicates the location (red box) relative to Lagoon Point, Bush Point, Greenbank, and Freeland.

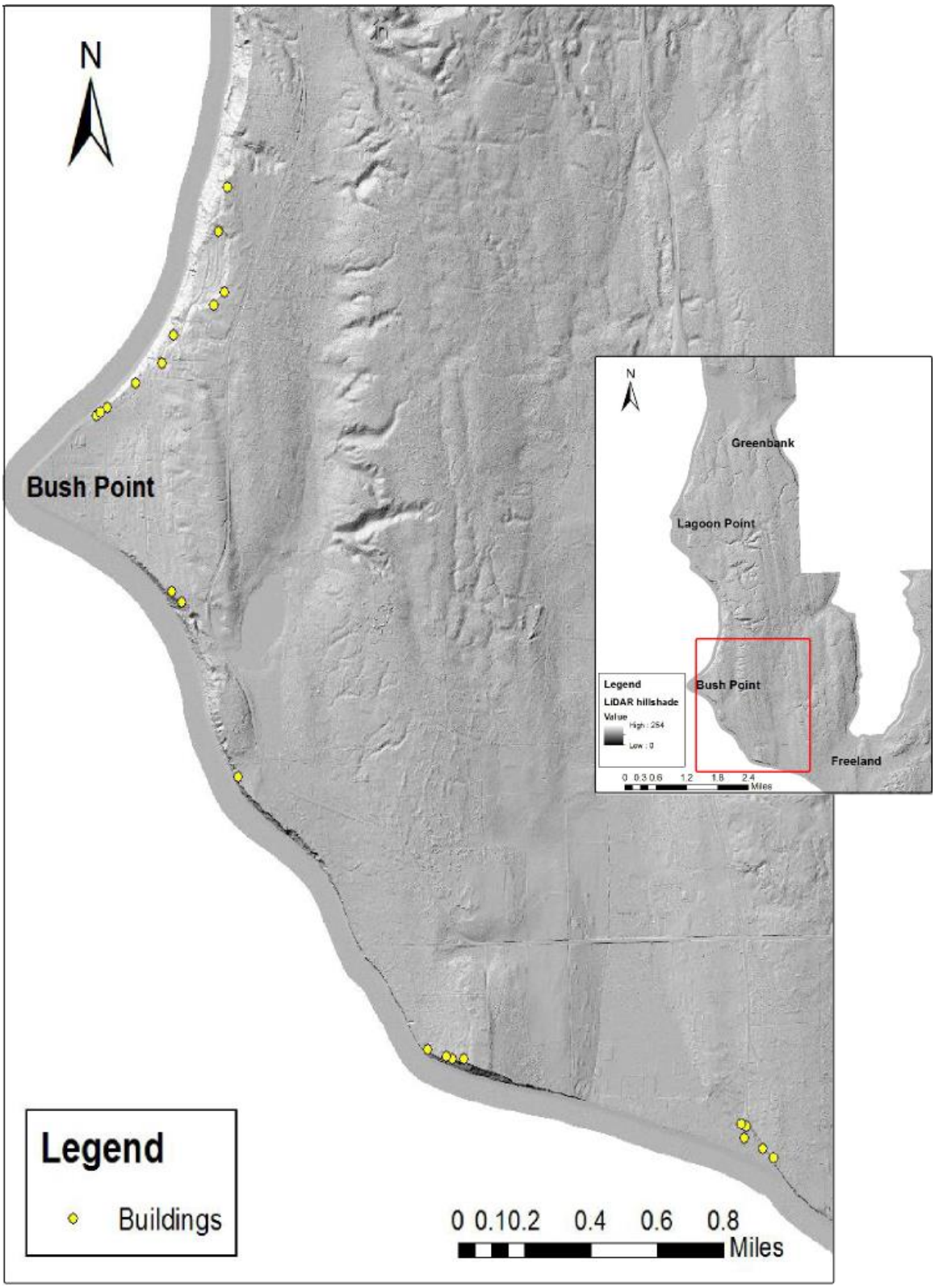

Figure 11b. Buildings (yellow points) that would be affected from a shallow landslide with a setback of 9 m and a runout of 60 m. Map on the left indicates the location (red box) relative to Lagoon Point, Bush Point, Greenbank, and Freeland.

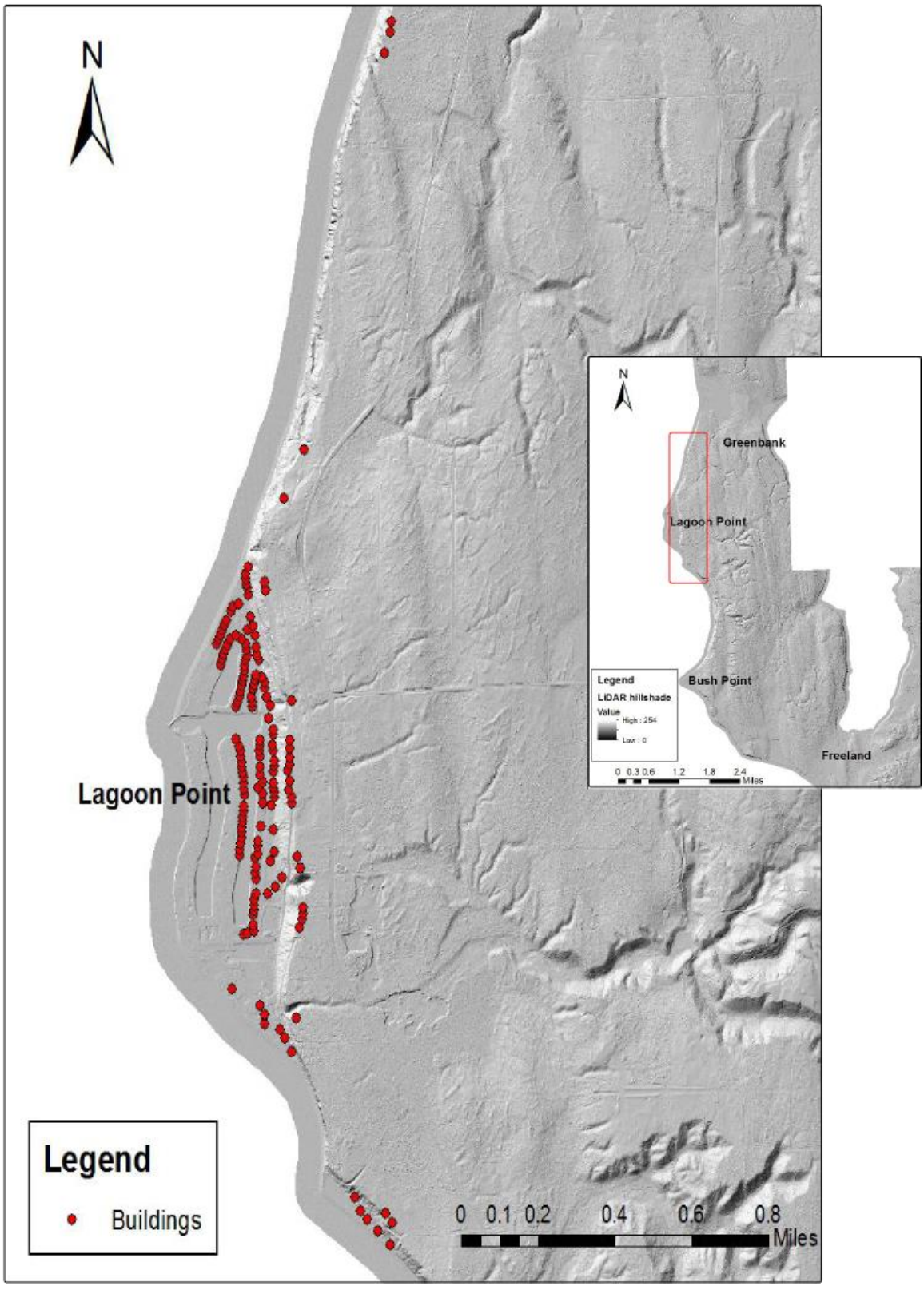

Figure 12a. Buildings (red points) that would be affected from a shallow landslide with a setback of 12 m and a runout of 235 m. Map on the left indicates the location (red box) relative to Lagoon Point, Bush Point, Greenbank, and Freeland.

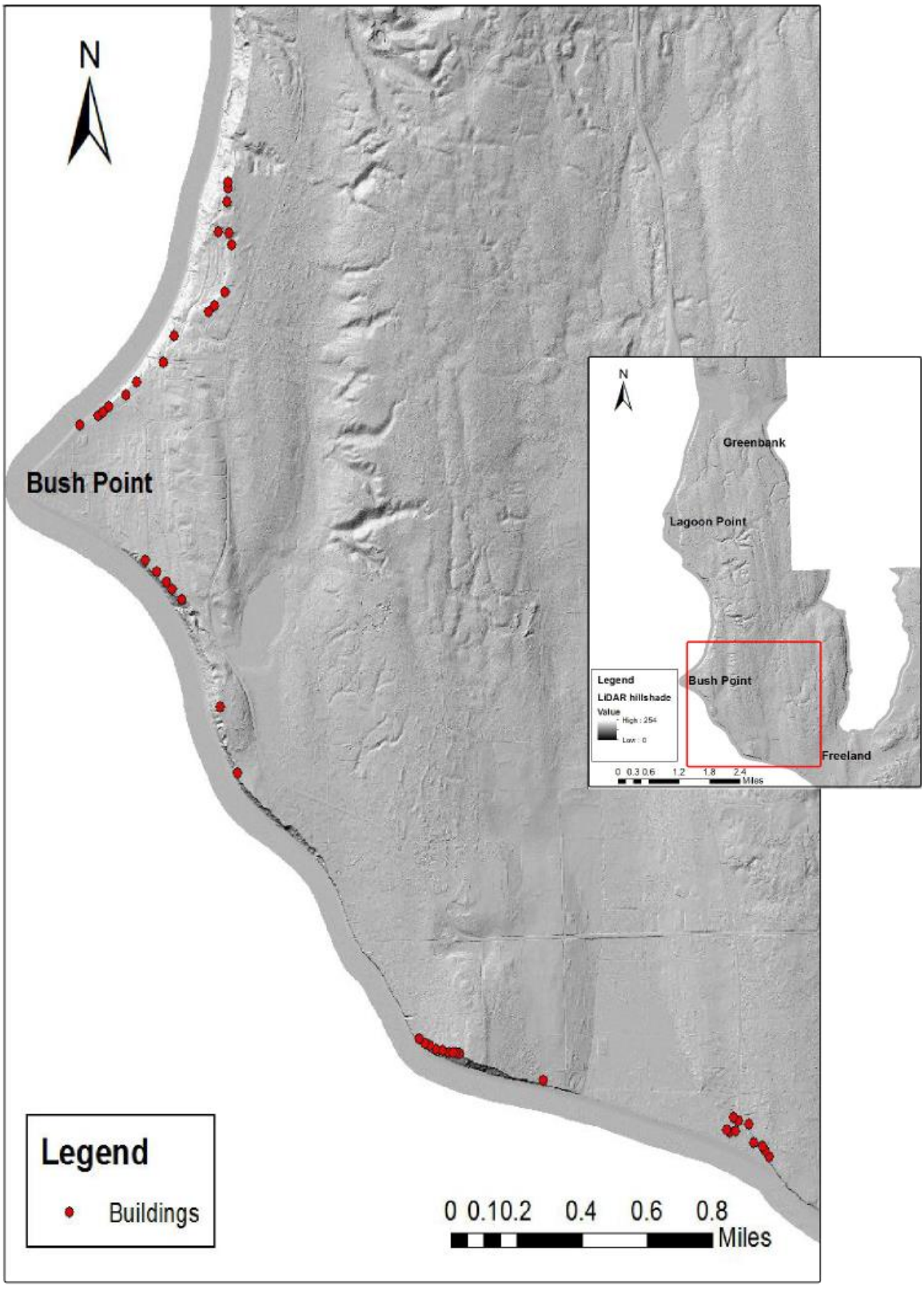

Figure 12b. Buildings (red points) that would be affected from a shallow landslide with a setback of 12 m and a runout of 235 m. Map on the left indicates the location (red box) relative to Lagoon Point, Bush Point, Greenbank, and Freeland.

Appendix

Density (number of landslides per 4 hectare count circle)	Mean Recurrence Interval (years)	Exceedance Probability (percent chance of one or more landslides during a specified time)					
		1 yr.	5 yrs.	10 yrs.	25 yrs.	50 yrs.	100 yrs.
1	88.40	1.12	5.50	10.70	24.63	43.20	67.74
2	44.20	2.24	10.70	20.25	43.20	67.74	89.59
3	29.47	3.34	15.61	28.78	57.19	81.67	96.64
4	22.10	4.42	20.25	36.40	67.74	89.59	98.92
5	17.68	5.50	24.63	43.20	75.68	94.09	99.65
6	14.73	6.56	28.78	49.27	81.67	96.64	99.89
7	12.63	7.61	32.69	54.70	86.19	98.09	99.96
8	11.05	8.65	36.40	59.54	89.59	98.92	99.99
9	9.82	9.68	39.89	63.87	92.15	99.38	100
10	8.84	10.70	43.20	67.74	94.09	99.65	100
11	8.04	11.70	46.32	71.19	95.54	99.80	100
12	7.37	12.69	49.27	74.27	96.64	99.89	100
13	6.80	13.68	52.06	77.02	97.47	99.94	100
14	6.31	14.65	54.70	79.48	98.09	99.96	100
15	5.89	15.61	57.19	81.67	98.56	99.98	100
16	5.53	16.56	59.54	83.63	98.92	99.99	100
17	5.20	17.49	61.77	85.38	99.18	99.99	100
18	4.91	18.42	63.87	86.95	99.38	100	100
19	4.65	19.34	65.86	88.34	99.54	100	100
20	4.42	20.25	67.74	89.59	99.65	100	100
21	4.21	21.14	69.51	90.70	99.74	100	100
22	4.02	22.03	71.19	91.70	99.80	100	100
23	3.84	22.91	72.77	92.59	99.85	100	100
24	3.68	23.78	74.27	93.38	99.89	100	100
25	3.54	24.63	75.68	94.09	99.91	100	100
26	3.40	25.48	77.02	94.72	99.94	100	100

Extension of Table 2 from Coe et al. (2000) Landslide densities, mean recurrence intervals, and probability (percent chance) of one or more landslides occurring during a specific time in the future. Exceedance probabilities of 100 percent have been rounded up from values that were greater than 99.995